

Dynamic Analysis of a Deep Groove Ball Bearing Using Finite Element Method

Ajay Mishra



Department of Industrial Design
National Institute of Technology Rourkela

Dynamic Analysis of a Deep Groove Ball Bearing Using Finite Element Method

*Thesis submitted to the
National Institute of Technology Rourkela
in partial fulfillment of the requirements*

*of the degree of
Masters of Technology*

in

Industrial Design

by

Ajay Mishra

(Roll Number: 214ID1390)

*under the supervision of
Prof. Dibya Prakash Jena*



May, 2016

Department of Industrial Design
National Institute of Technology Rourkela

Declaration of Originality

I, Ajay Mishra, Roll Number 214ID1390 hereby declare that this thesis entitled "*Dynamic Analysis of A Deep Groove Ball Bearing Using Finite Element Method*" represents my original work carried out as a postgraduate student of NIT Rourkela and, to the best of my knowledge, it contains no material previously published or written by another person, nor any material presented for the award of any other degree or diploma of NIT Rourkela or any other institution. Any contribution made to this research by others, with whom I have worked at NIT Rourkela or elsewhere, is explicitly acknowledged in the thesis. I have also submitted my original research records to the scrutiny committee for evaluation of my thesis.

I am fully aware that in the case of any non-compliance detected in future, the Senate of NIT Rourkela may withdraw the degree awarded to me by the present thesis.

May 26, 2016

NIT Rourkela

Ajay Mishra

Acknowledgement

First of all, I would like to express my deepest gratitude to my supervisor, **Prof. Dibya Prakash Jena**, for his support and guidance. I am thankful to **Mr. Salkhu Marandi** for supporting me in my lab work and all my classmates at NIT for a nice working environment.

At last, I would like to thank my friends and family for all support and encouragement throughout the project and also during my years as a student at NIT Rourkela.

May 26, 2016
NIT Rourkela

Ajay Mishra
Roll Number: 214ID1390

Abstract

In present work, a deep groove ball bearing commonly known as rolling element bearing (REB) has been analyzed using finite element method (FEA). Vibration response has been extracted in the y-direction and used to estimate the bearing characteristic frequencies. In past two decades, defects have been analyzed using vibration response collected from experimental setup. When rolling element pass through the defect, an impact load transmitted through the bearing part to the surface of the bearing housing. Dynamic analysis of the bearing has the capability to analyze the bearing while in motion and calculate the stress developed in each part of the bearing as well as extraction of the vibration signal.

In this piece of research, dynamic analysis of a deep groove ball bearing is conducted using finite element method (FEA) without and with known defect. For simulation, a widely used bearing with model number W-6206 2Z has been taken into consideration which is very common in 3-wheeler automobiles. Two models have been modeled in the simulation software ANSYS 15.0. The first model designed with a healthy bearing and a three support system whereas the second model with the known defect i.e. wear in the outer race inner surface. In the simulation of the first model, various boundary conditions have been given in the simulation software ANSYS 15.0 to find the rotation of the bearing model W-6206 2Z. Vibration signals extracted from this analysis have been further analyzed. The second model with known defect, which has been made at the inner surface of the outer race has been exposed to the same boundary conditions. Faulty signature has been found, when the ball rolled over the known defect, monitored from the signals captured by an accelerometer.

Keywords: Rolling element bearing; outer race defect; Finite element method.

Contents

DECLARATION OF ORIGINALITY	III
ACKNOWLEDGEMENT	IV
ABSTRACT	V
LIST OF FIGURES.....	VIII
1 INTRODUCTION	1
1.1 BEARING	1
1.2 TYPES OF BEARING	2
1.2.1 Plain Bearing	2
1.2.2 Rolling Bearing	2
1.2.3 Jewel Bearing	3
1.2.4 Fluid Bearings	4
1.2.5 Magnetic Bearing	4
1.2.6 Flexure Bearing	5
1.3 BALL BEARING	5
1.3.1 Geometry and Elements of Deep Groove Ball Bearing	6
1.3.2 Advantages and Limitations.....	6
1.4 OBJECTIVES	7
1.5 LITERATURE REVIEW	7
2 THEORETICAL ASPECTS OF THE WORK	10
2.1 FINITE ELEMENT METHOD	10
2.2 NONLINEAR ANALYSIS	10
2.2.1 Changing Status.....	11

2.2.2	Geometric Nonlinearities	11
2.2.3	Material Nonlinearities.....	12
3	TRANSIENT DYNAMIC ANALYSIS.....	13
3.1	TYPES	15
3.2	STAGES OF TRANSIENT ANALYSIS	15
3.2.1	Build the Model.....	16
3.2.2	Apply Loads and Obtain the Solution	16
3.2.3	Review the Results	18
4	MODELLING.....	19
4.1	FIRST MODEL.....	19
4.2	INTERMEDIATE MODELS	21
4.3	FINAL MODEL	21
4.3.1	Modelling in ANSYS 15.0.....	22
4.4	SUPPORT SYSTEM	24
4.5	MODEL MESHING IN ANSYS 15.0.....	25
4.6	MODEL WITH CRACK	26
5	RESULTS AND DISCUSSION.....	27
6	CONCLUSION.....	30
6.1	SCOPE FOR FUTURE RESEARCH.....	30
	REFERENCES	31
	ANNEXURE – A.....	33

List of Figures

1.1: Plain bearing	2
1.2: Rolling element bearing (a) ball and (b) cylindrical	3
1.3: Jewel bearing	3
1.4: Fluid bearing.....	4
1.5: Magnetic bearing	4
1.6: Flexure bearing (hinge in a Tic-Tac box).....	5
1.7: Structure of a typical deep groove ball bearing	6
2.1: A fishing rod demonstrates geometric nonlinearity	11
2.2: Stress-strain curve for ductile material.....	12
4.1: Sketch of bearing no. 6310	19
4.2: Dimensions in CATIA V6 for ball bearing no. W-6310	20
4.3: CATIA model of ball bearing no. W-6310	20
4.4: Dimensions of bearing W 6206-2Z	21
4.5: Model of bearing in ANSYS 15.0	22
4.6: Final design of cage	23
4.7: Final model of bearing in ANSYS 15.0	23
4.8: Modelling of three support system in ANSYS15.0.....	24
4.9: Final model of ball bearing setup with support system n ANSYS 15.0.....	24
4.10: Model meshing in ANSYS15.0.....	25
4.11: Second model (bearing with crack).....	26
5.1: Positions of accelerometers probe in the model	27
5.2: Vibration response of healthy bearing with frequency (1000,3000 and 5000 Hz)	28
5.3: Vibration response of bearing with defect with frequency (1000,3000 and 5000 Hz)29	29

Chapter 1

Introduction

In industries and general life, the typical rotating machinery generates serious vibrations and causes the downgrading of the system or creates a noisy and unhealthy environment. Household appliances like washing machine, mixer, and air conditioner are made noiseless for the user compatibility. The source of the noise is the electric motor fitted with this machinery. The typical element that causes it to rotate is Bearing. Now a day's bearings are improved to emit low noise and vibrations as per the users' comfort. What thereby noise generates by the bearing is becoming the decisive factor for the bearing acceptance as well as designing.

It is very important to develop an improved system for monitoring the condition of the bearing which is cost effective, reliable and to overcome the conventional method like the periodic shutdown of the machinery for preventive maintenance. Any industrial rotating machinery like turbine typically depends on bearings and fails to perform action completely when a bearing is undergone a severe defect. So condition monitoring is a major aspect regarding the rotating machinery and has to be done before it causes catastrophic breakdown of the machinery.

In gearbox, vibration signals are the resultant vibrations coming from gears meshing as well as the bearing. So any device which is used for extracting the vibration signal gives the compound vibration or mixed vibration. For calculating individual vibration coming from bearing it is to be done individually and therefore an improved monitoring system is required.

1.1 Bearing

Moving component i.e. bearing, most likely called a Rolling bearing, is a machine element which takes a load by putting moving components, (for example, balls or rollers) between two bearing rings called races. The relative movement of the races causes the moving parts to move with very little rolling resistance and with small sliding.

1.2 Types of Bearing

There are six common types of bearing. Each works on a different principle.

1.2.1 Plain Bearing

It is the simplest form of bearing in which a shaft makes surface contact with the bearing surface. The relative motion between bearing and the journal (contact surface area of the shaft with bearing) is nothing but the sliding motion between the two surfaces (fig: 1.1).



Figure 1.1: Plain bearing [1]

1.2.2 Rolling Bearing

Rolling element bearing also called as rolling bearing comprises of basically inner ring, outer ring and rolling element. Rolling bearing has two types of contacts i.e. point contact (deep groove ball bearing) and line contact (cylindrical roller bearing). It exhibits low friction between races and rolling element and helps in reducing cost, weight, capacity, durability, size, etc. Contact surfaces are hardened to provide smooth operation (fig: 1.2).

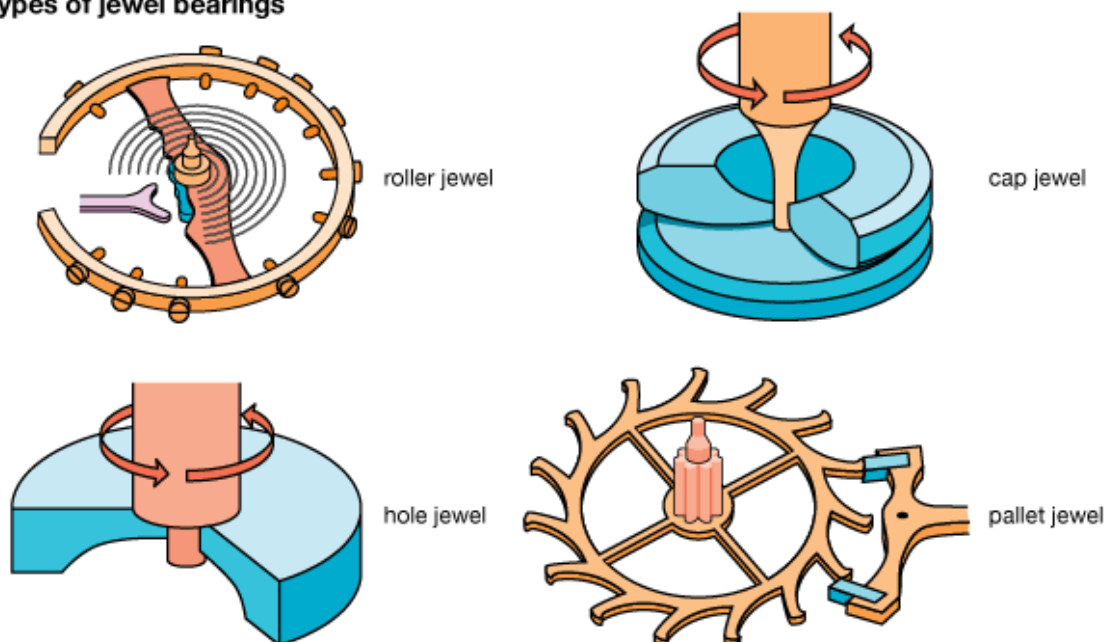


Figure 1.2: Rolling element bearing (a) ball [2] and (b) cylindrical [3]

1.2.3 Jewel Bearing

Jewel bearing is the type of plain bearing in which a spindle rotates in jewel lined hole. The diameter of the hole is usually larger than the spindle. The most common material for jewel bearing is Ruby. Jewel bearing is typically used in watches where very low friction, as well as long life span, is required. It is used where dimensional accuracy is essential like in precision instruments. A common type of jewel bearing is listed in fig: 1.3.

Types of jewel bearings



© 2012 Encyclopædia Britannica, Inc.

Figure 1.3: Jewel bearing [4]

1.2.4 Fluid Bearings

Fluid bearings are the bearings that carry their loads using a thin layer of fluid or air between the rings. These bearings are used wherein high-load and high-speed operations, in which other forms of bearings fail to operate. They are commonly classified as fluid dynamic and hydrodynamic bearing (fig: 1.4).

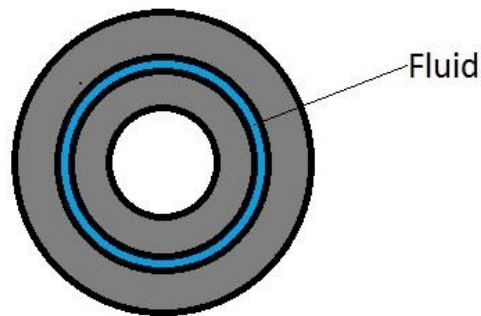


Figure 1.4: Fluid bearing [5]

1.2.5 Magnetic Bearing

These bearings are the bearings which permit no physical contact between outer and inner ring as the rotation is possible with a magnetic induction between the two rings. Some magnetic bearings (fig: 1.5) use a permanent magnet, therefore, no external power source is required for transmission of loads, but they are difficult to design.

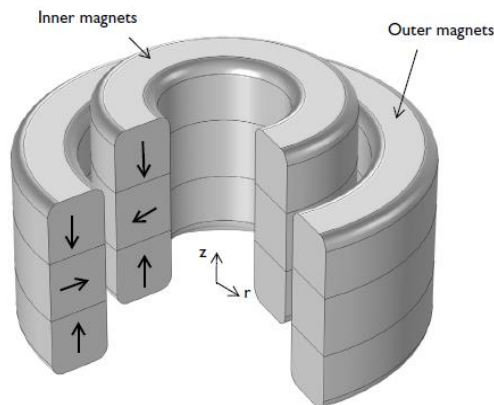


Figure 1.5: Magnetic bearing [6]

1.2.6 Flexure Bearing

Flexure bearings (fig: 1.6) are the bearings by which motion is transmitted through bending of a load element. These bearings are very cost efficient and easy to construct. They exhibit very low friction.



Figure 1.6: Flexure bearing (hinge in a Tic-Tac box) [7]

1.3 Ball Bearing

The ball bearing is the element of the machine which gives relative (rotary) motion between two parts i.e. shaft or hub and the bearing casing. The main objective is to lower the rotary resistance (rotational friction) between moving parts by providing point contacts through metal spheres or balls. Ball bearing supports axial and radial loads. It is achieved by providing a rolling element (metal balls) between the races to transmit the loads. It is used in two ways i.e. by fixing one of the races and rotating the other race to transmit the load. In most of the application, the outer race is fixed to the bearing casing and inner race moves with the rotating shaft. Ball bearings are cheaper than the cylindrical roller bearing as it uses balls in place of cylinders and construction point of view. Balls bearing are different types such as axial, angular contact, thrust, and deep groove ball bearing.

1.3.1 Geometry and Elements of Deep Groove Ball Bearing

A typical deep groove ball bearing consists of four parts i.e. inner race, outer race, rolling element (balls) and cage. In the inner ring and outer ring, grooves are provided in a guideway for the rolling motion of the balls and also constraining the motion of the balls. Cage is provided to maintain a minimum distance between balls, to reduce the number of balls thus lowering the weight of the bearing and to lowering the friction by creating a convex-concave contact instead of convex-convex contacts. This type of contact also avoids dents on the balls and hence improve the lifespan of the bearing. A typical deep groove ball bearing is listed in fig: 1.7.

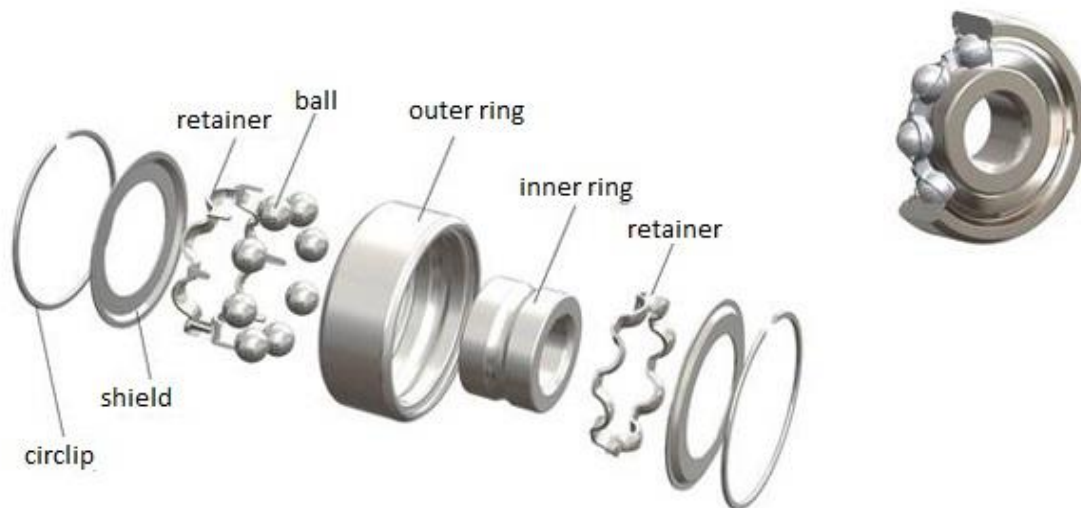


Figure 1.7: Structure of a typical deep groove ball bearing [8]

1.3.2 Advantages and Limitations

Deep groove ball bearing is mainly used for supporting the purely radial load and also to support both axial and radial load. If it is to support a large axial load, then angular contact bearings are used. With larger radial clearance it can withstand high speed and also its friction coefficient is less. In the large axial loading conditions, deep groove ball bearing has advantages over thrust angular ball bearing. It has many advantages like cost effective, durability, high-speed, low maintenance, etc. and is the most widely used bearing in the industrial applications.

The main limitation of that deep groove ball bearings is the flattened balls over the large pressure on the outer ring that can lead to the bearing failure. So load ratings and monitoring of the bearing is very important.

1.4 Objectives

- The main objective of this research work is to design a bearing and find the rotation of the bearing in ANSYS 15.0.
- Second objective is to extract the vibration response from both healthy bearing as well as bearing with fault.

1.5 Literature Review

Shiroishi *et al.* [9] investigated detection methods for rolling element bearing defects by means of signature sensor analysis, especially the use of a modern signal processing mixture of the high-frequency resonance method and adaptive line enhancer technique. The accelerometer, transducers, and the acoustic emission sensors are used to obtain data for the analysis. Experimental results are gained for the defects in outer race and inner race. Results show the efficiency of the signal processing technique to conclude both the harshness and defect location. So this gives a direction to find out it mathematically.

Yuh-Tay Sheen *et al.* [10] proposed a complex filter for Hilbert transform to apply in the demodulation of operating vibration signals. The filter from Hilbert transform could deliver the complex signal unswervingly, as the function of time and frequency, so the envelope can be obtain from the total measure of the complex signals. The parameters such as the center frequency, scaling factor, and the passband width, are entertained to reach the appropriate possessions of fast waveforms convergence, little phase distortion and the continuous passband improvement, and thus, a restricted waveform interim of the projected filter can be possibly functional in the area of demodulation of vibration signal.

Graney *et al.* [11] performed an analysis to show the reliance of discrete frequency indicators, acceleration time-waveform crest factor, velocity amplitude, acceleration time-waveform characteristics and high-frequency natural bearing resonance indicator on the rolling element bearing health. They described the four stages of the wear and concluded that wear occurrence is random in nature and strongly depend on the lubricant and the

nature of the dynamic forces applied to the bearing. Bearing fundamental frequencies have been calculated for validating the results.

Pandiyarajan.R *et al.* [12] determine the contact stress of large diameter bearings using numerical and analytical methods. Sectional analysis has been performed to overcome the problems of CPU timing and the memory management. Hertzian Elliptical Contact Theory has been used to find out the contact stress in the analytical method. Maximum contact pressure has been calculated using finite element method and also analyzed at the contact zone of the balls and the raceway to predict the contact pressure. Validation has been done by comparing the stresses find out by analytical with the numerical methods.

According to Kharche *et al.* [13] that Defective bearings are the source of vibrations in machines. Due to constructional features of bearing, they generate vibrations. As the condition of bearings changes during use, the nature of vibrations also changes and it has definite characteristics depending upon the cause. This characteristic feature of bearing makes them suitable for vibration monitoring. It is a review paper for fault detection technique in rolling element bearing; it covers rolling element bearing components and its geometry, bearing failure modes, bearing condition monitoring techniques, time domain, and frequency domain techniques.

S. G. *et al.* [14] presented focuses upon the detection of a localized defect in a taper roller bearing using vibration analysis. For bearing analysis, frequency domain approach is taken followed by experimentation for the detection of vibration signal in which single point defects are artificially created on roller and outer race, then for vibration response these defected taper roller bearings are tested under different speed and loading conditions, and resulting vibration signals are then processed using considered vibration-based techniques in frequency domain. Bearing vibration signature analysis is used as a medium for fault detection. Finally, the results are then compared to healthy bearing vibration response. Extracting characteristic defect frequency obtains the identification of the bearing defect from vibration signal of the defective bearing. Conclusions are drawn about the effective vibration monitoring of bearings.

Saruhan *et al.* [15] performed an experiment in which one test bearing has taken with different conditions such as no defect, outer race defect, inner race defect, ball defect and the combined rolling element defects. Bearings tested on two loading conditions and with different operating frequencies and four different rotating speeds. The vibration data collected by the mean of two accelerometers fitted to the bearing housing and with relative

spacing of 90° angle and used for the purpose of authentication is composed of four different defects states of the rolling element bearing. The bearing characteristic frequencies calculated by simply multiplying the frequency multipliers such as ball pass frequency multiplier of the outer race, ball pass frequency multiplier of the inner race and ball spin frequency multiplier with the shaft rotational speed. The equations used for calculating these multipliers are as following.

$$BPFI = \left(\frac{N_b}{2} \right) \left(1 + \left(\frac{N_b}{d_p} \right) \cos \alpha \right) \quad 1.1$$

$$BPFO = \left(\frac{N_b}{2} \right) \left(1 - \left(\frac{N_b}{d_p} \right) \cos \alpha \right) \quad 1.2$$

$$BSF = \left(\frac{D_p}{2d_b} \right) \left(1 - \left\{ \left(\frac{d_p}{d_b} \right) \cos \alpha \right\}^2 \right) \quad 1.3$$

Where BPFI is ball pass frequency multiplier of the inner race, BPFO is ball pass frequency multiplier of the outer race, BSF is ball spin frequency multiplier, N_b is number of rolling elements, d_p is pitch diameter, d_b is rolling element diameter, and D is contact angle which is the angle of load from the radial plane. The results obtained from the experiments have been validated with the numerical data.

Bajaj *et al.* [16] did FEA analysis of bearing for proposing the design of an integral shaft bearing. Structural and thermal analysis have been performed to find out the characteristic properties of the bearing. Heat flow has been analyzed through the temperature distribution and stress concentration. The performance of the bearing has been characterized mainly by thermal elongation due to friction and the stress concentration between the rolling element and the raceway. The effects of the thermal elongation on the clearance has also been analyzed.

Chapter 2

Theoretical Aspects of the Work

In the present work, the finite element method is used with CATIAV6 modelling software and ANSYS 15.0 academic research modelling and analysis software. The ongoing chapter gives a concise knowledge of the workspace and methodology and related terms to the user provided the user has some basic knowledge of modelling in CATIA V6 and application of ANSYS 15.0 modelling and analysis module for applying boundary conditions.

2.1 Finite Element Method

A finite element method is a powerful tool that comprises of numerical methods for calculating the solutions to the problems that are governed by elliptical partial differential equations. In this method, the whole model is divided into some elements and nodes that have some basic element types and definite nodes. The load is transferred from node to node and stress concentration, strain observation and total deformations can be easily calculated by the governing calculations. With the help of simulation software that uses FEA, it is easy to capture the nodal force and stress with the proper visualization.

2.2 Nonlinear Analysis

Nonlinear analysis is nothing but the non-linear behavior of the stress, strain or deformation with the applied load and boundary conditions.

There are many causes of nonlinearity which can be categorized into three categories:

2.2.1 Changing Status

Many structures exhibit nonlinearity due to change of status abruptly from no contact to contact, and so they are status dependent. For example, a rope's behavior changes from slack to tight or a rolling surface changes from no contact to contact. It can be easily understood by the spring system (fig: 2.1).

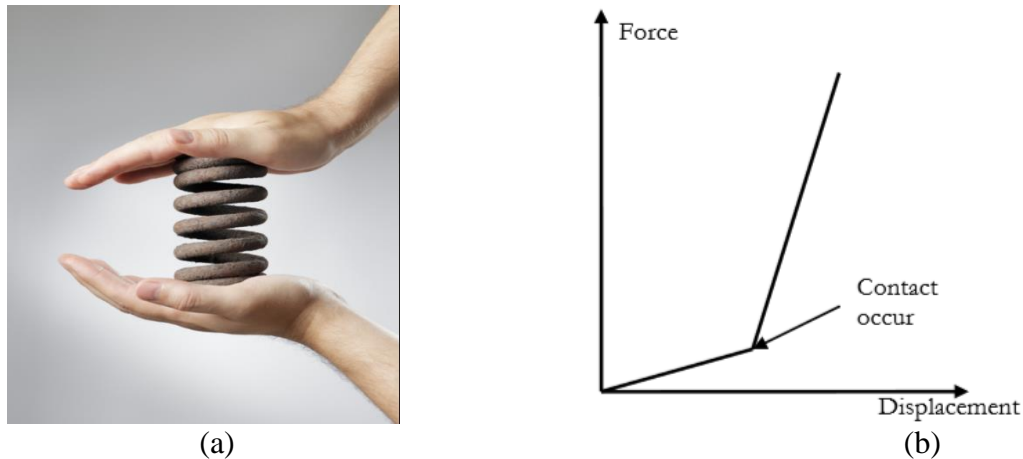


Figure 2.1: (a) Spring nonlinearity from no contact to contact [17], (b) Force vs. displacement behavior [18]

2.2.2 Geometric Nonlinearities

Geometric nonlinearities occurred when some bodies underwent a large deformations or rotations with the application of load. The very common example of this type of nonlinearity is the behavior of fishing rod (fig: 2.2).

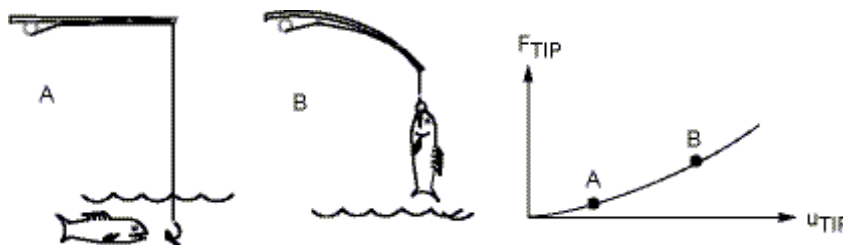


Figure 2.1: A fishing rod demonstrates geometric nonlinearity [19]

2.2.3 Material Nonlinearities

The behavior of stress-strain (fig: 2.3) is the common cause of material nonlinearities. Many factors affect this behavior like repeatedly applied a load, long applied load cause creep.

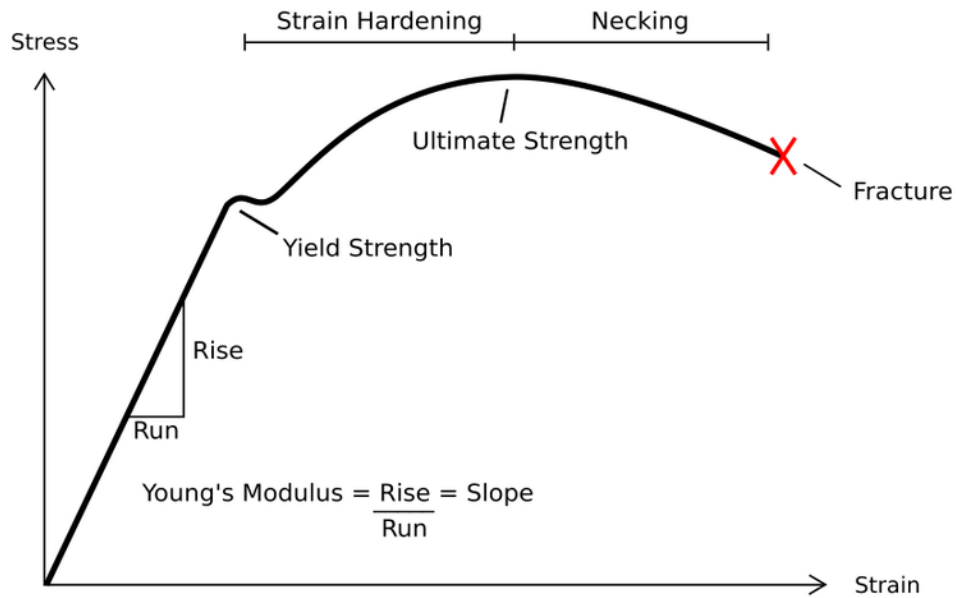


Figure 2.2: Stress-strain curve for ductile material [20]

Chapter 3

Transient Dynamic Analysis

The transient dynamic analysis is the best method to find out the dynamic response of any structure, under the action of any general time-dependent loads. This analysis is basically used to define time-varying displacements such as strains, stresses, and forces in any structure and all combination of loads such as static, transient, and harmonic loads. To evaluate the response of deformable bodies with inertial effects transient, structural analyses is very significant. When inertial and damping effects are not considered then, a linear or nonlinear static analysis is done. For a sinusoidal and linear response, a harmonic response analysis is done. The rigid dynamic analysis is done for rigid and the kinematics bodies. Generally, in most cases dynamic analysis is done. In this analysis, it is necessary to consider inertia or damping effects. If there is no inertia and damping effects, then static analysis use in place of dynamic analysis. The equation (IV) used to find transient dynamic analysis is:

$$[M]\{\ddot{u}\} + [C]\{\dot{u}\} + [K]\{u\} = \{F\} \quad 3.1$$

where:

[M] stands for mass structural matrix

[C] stands for structural damping matrix

[K] stands for structural stiffness matrix

$\{\ddot{u}\}$ stands for nodal acceleration vector

$\{\dot{u}\}$ stands for the nodal velocity vector

$\{u\}$ stands for the nodal displacement vector

$\{F(t)\}$ stands for load vector

- For analysis of transient response damping matrix may be used. It can be represented in the following manner:

$$\begin{aligned}
[C] = & \alpha[M] + \beta[K] + \sum_{i=1}^{N_{ma}} \alpha_i^m [M_i] + \sum_{i=1}^{N_{ma}} \sum_{k=1}^{N_{sa}} \alpha_p [M_k]_i + \sum_{j=1}^{N_{mb}} \beta_j^m [K_j] \\
& + \sum_{j=1}^{N_{ma}} \sum_{n=1}^{N_{sb}} \beta_q [K_n]_j + \sum_{k=1}^{N_e} [C_k] + \sum_{l=1}^{N_g} \beta_q [G_l]
\end{aligned} \tag{3.2}$$

Where,

$[C]$ stands for structural damping matrix

α stands for mass matrix multiplier

$[M]$ stands for structural mass matrix

β stands for stiffness matrix multiplier

$[K]$ stands for structural stiffness matrix

N_{ma} stands for the number of materials with MP, ALPD input

α_i^m stands for the number of materials

$[M_i]$ stands for a portion of structural mass matrix based on material i

N_{ma}^{MD} stands for the number of elements with mass proportional material damping input

N_{sa} stands for the number of sections in an element with mass proportional material damping input

α_p stands for mass proportional material damping factor for section point K with material P

$[M_k]_i$ stands for a portion of element i structural mass matrix based on section K

N_{mb} stands for the number of materials with MP, BETD input

β_j^m stands for stiffness matrix multiplier for material j (input as BETD on the MP)

$[K_j]$ stands for a portion of the structural stiffness matrix based on material j

N_{ma}^{MD} stands for the number of elements with stiffness proportional material damping input

N_{sb} stands for the number of sections in an element with stiffness proportional material damping input

β_q stands for stiffness proportional material damping factor for section point n with material

$[K_n]_j$ stands for a portion of element j structural stiffness matrix based on section n

N_e stands for the number of elements with specified damping

$[C_k]$ stands for element damping matrix

N_g stands for the number of elements with Coriolis or gyroscopic damping

$[G_l]$ stands for element Coriolis or gyroscopic damping matrix

3.1 Types

There are two types of dynamic analysis, Implicit, and Explicit. Both are time integration approaches used to perform dynamic simulations Solution. The main difference between Implicit and Explicit are the type of contact. In Implicit dynamics, all contacts must be defined before solving wherein explicit dynamics there is no need to define non-linear contacts before solving materials. Also in explicit dynamics, material failure models support more than in implicit dynamics.

3.2 Stages of Transient Analysis

The main stages of this analysis are:

1. Build the model.
2. Apply loads and obtain the solution.
3. Review the results.

3.2.1 Build the Model

This is the first step of the analysis. In this step, identification of job name and analysis title is made. To describe the element types, real element constants, material properties, and the model geometry, PREP7 is used. The ANSYS Modeling and Meshing Guide explains them in detail. The following points must be considered in this step:

- Use both linear and nonlinear elements.
- Both Young's modulus (EX) and density (DENS) must be defined. Material properties may be linear or nonlinear, isotropic or orthotropic, and constant or temperature-dependent.

Following parameters are important for mesh density:

- Fine meshing should be done to determine the parameters such as load, deformation, etc. at the area of highest stress concentration.
- More fine mesh requires in the regions of stresses or strains in compare to the regions where only displacements are required.
- The mesh should be able to detect the effects of the nonlinearities. For example, the reasonable integration point density requires for plasticity.
- The mesh should also be fine enough to resolve the wave in wave propagation effects.

3.2.2 Apply Loads and Obtain the Solution

The second step is to initiate the finite element solution in which we define the analysis type in options, apply loads and specify load steps.

This step is done in the following manner:

- a) Enter the ANSYS solution processor.
- b) Apply loads on the selected area or node.
- c) Apply supports wherever required,
- d) Set the appropriate and necessary boundary conditions required.

To define the highest mode of interest, a primary model analysis should be achieved before the transient structural analysis. It is important to observe the several mode shapes for determining highest mode frequency. Initial Conditions such as initial displacement and initial velocity are essential for transient structural analysis. In ANSYS default, the initial condition is set as all bodies are at rest. When some bodies have zero initial displacement but non-zero constant initial velocity then only bodies can be specified and enter constant initial velocity. Time-Varying Loads Structural loads and joint conditions can be input as time-dependent load histories. When adding a Load or Joint Condition, the magnitude can be defined as a constant, tabular value, or function. These values can be entered directly in the Workbench.

- **Defining Time Step**

To signify the dynamic response, it is important to use automatic time-stepping, proper selection of the initial, minimum, and maximum time steps accurately. Explicit time integration uses for rigid dynamic analyses and implicit time integration use for transient structural analyses. So we can say the time steps for transient structural analyses are larger. In dynamic response, numerous mode shapes of the assembly are important. It must practice automatic time-stepping. The choice of the time step is based on accuracy. In primary time step, this value can be the same or slightly higher. To avoid workbench, the minimum time step can be the input.

- **Automatic Time Stepping**

Automatic time stepping also refer as time step optimization. Its main work is to reduce the total number of time step by changing the size of time step which is based on response frequency and nonlinearities. It increases the loads automatically if any nonlinearity is present. For initializing automatic time stepping AUTOTS command is used.

Automatic time stepping is good for most of the analysis but there are some cases where it is not used.

- Problems having localized dynamic behavior such as hub assembly and turbine blade.
- Problems with continually changing time steps.
- Problems of kinematics consisting of rigid-body motion.

3.2.3 Review the Results

The results of the transient analysis have been written into the file *Jobname.RST*. It consists of the following data:

- Primary data
 - Nodal displacements (UX, UY, UZ, ROTX, ROTY, ROTZ)
- Derived data
 - Nodal and element stresses
 - Nodal and element strains
 - Element forces
 - Nodal reaction forces etc.

Chapter 4

Modelling

Several models have been prepared and tested on ANSYS15.0 by exporting. These models have undergone some errors, so they modified and tested several times to find the desired results. Modelling is done in Academic CATIA V6 software and ANSYS 15.0 and then exported to ANSYS 15.0 for simulation.

4.1 First Model

The first model that is modelled in CATIA V6 has following steps in modelling:

I. Selection of the Model and Defining the Dimensions of the Bearing

W-6310 has been selected and then hand sketch has been prepared with proper dimensions (fig: 4.1).

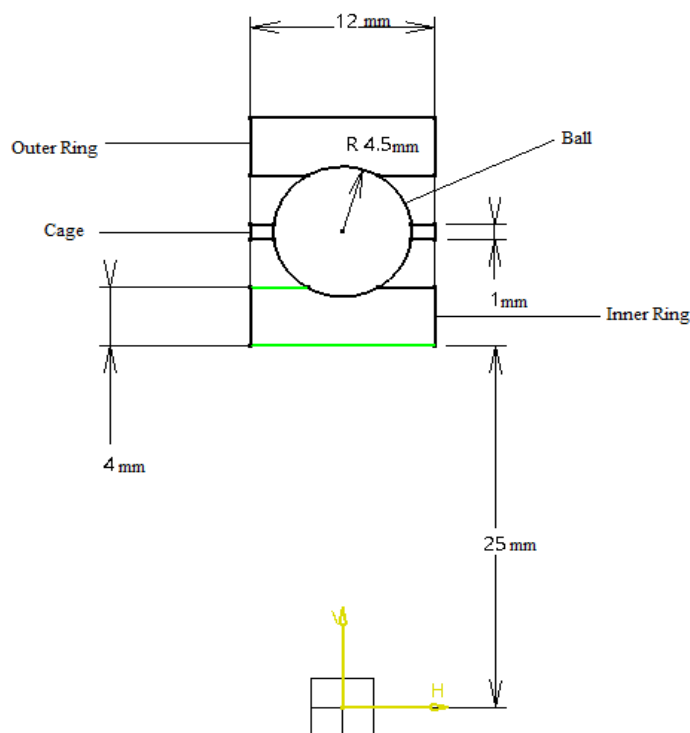


Figure 4.1: Sketch of bearing no. 6310

- II. CATIA V6 model has been prepared with accurate dimensioning and constraints (fig:4.2,4.3).

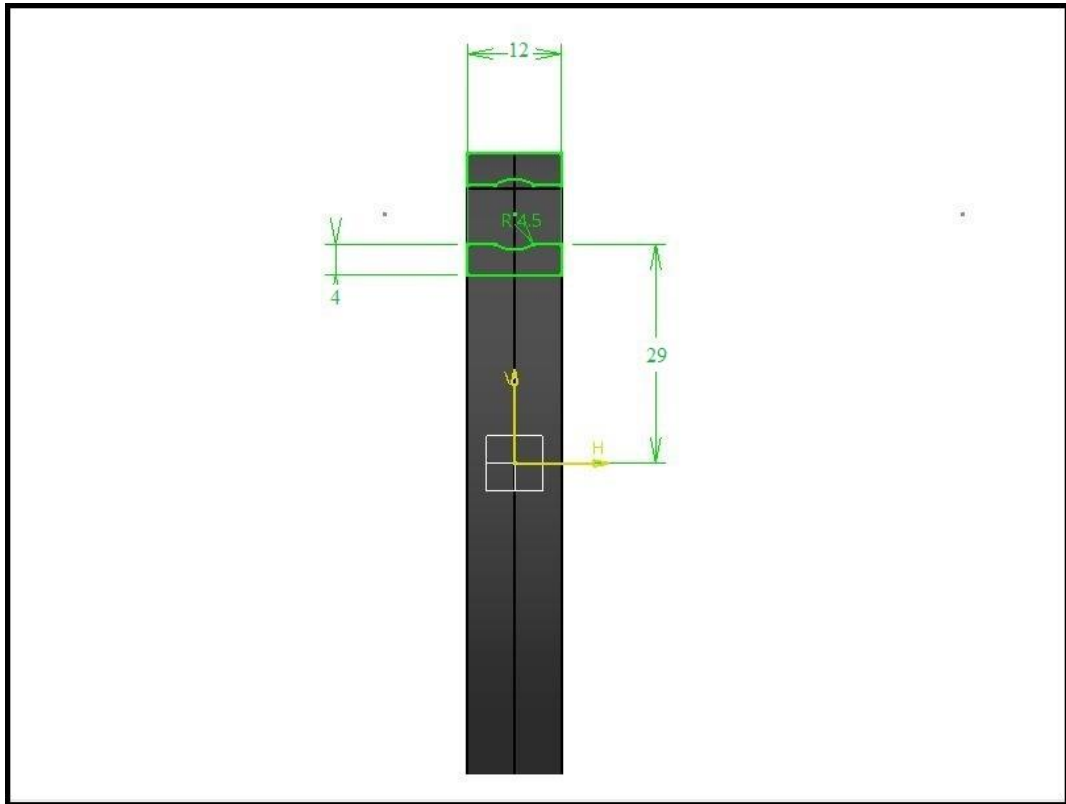


Figure 4.2: Dimensions in CATIA V6 for ball bearing no. W-6310

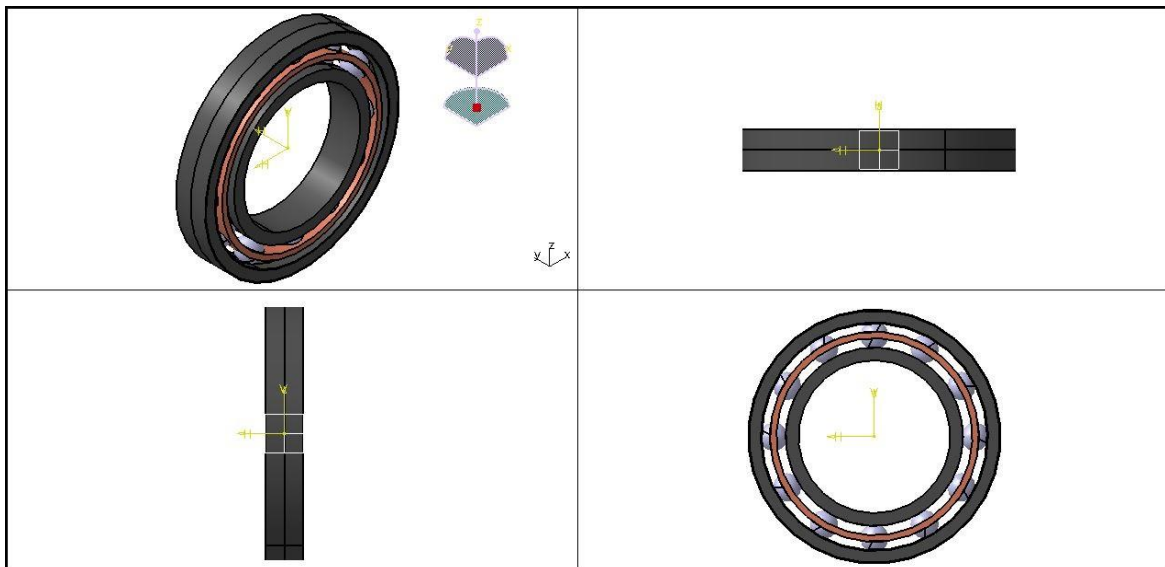


Figure 4.3: CATIA model of ball bearing no. W-6310

4.2 Intermediate Models

Some intermediate models have been prepared for finding the rotations, but they failed to rotate and therefore resulting in the appropriate model.

4.3 Final Model

After many tests, a bearing design is finalized which is used for simulation in ANSYS 15.0. Bearing model no. W-6206 2Z has been selected and modeled in ANSYS 15.0 modelling module only to overcome the errors. Its dimensions are listed in fig: 4.4.

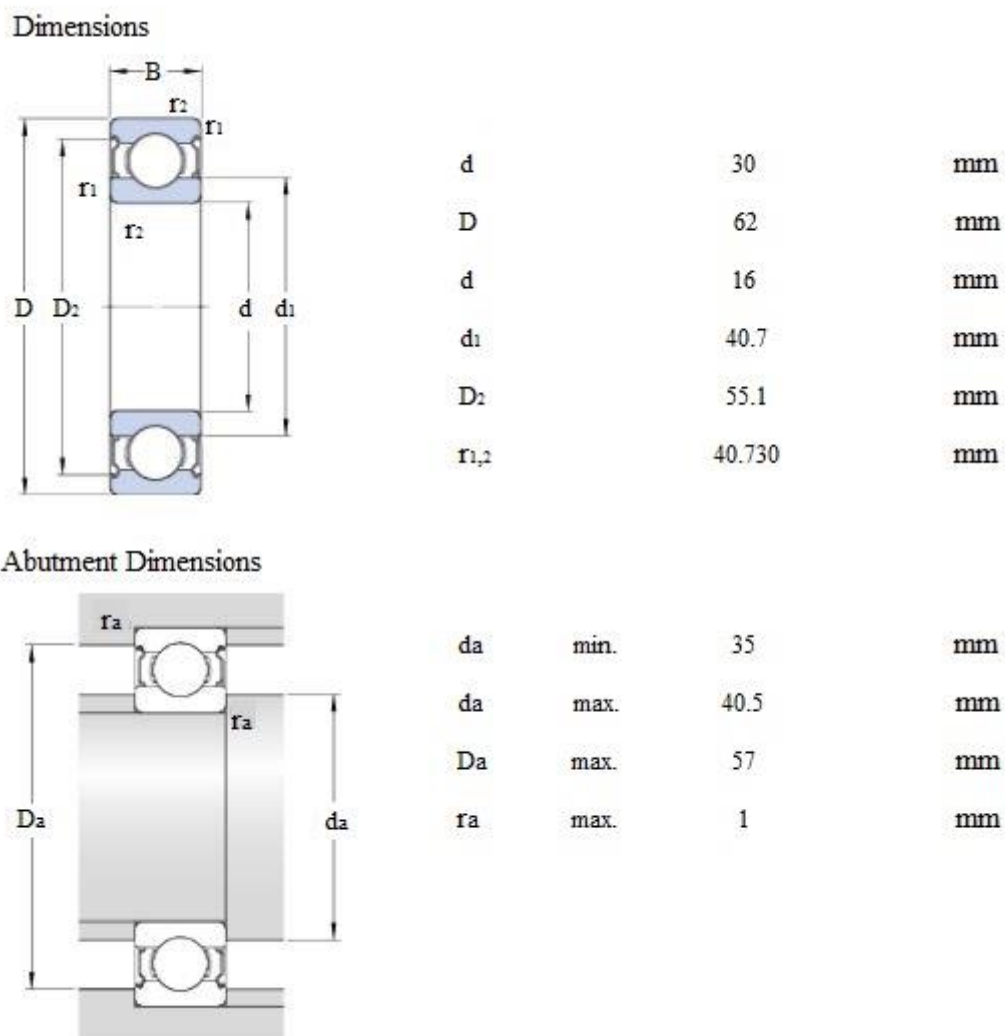


Figure 4.4: Dimensions of bearing W 6206-2Z [21]

Two models have been modeled with same bearing one is without defect and with a defect.

4.3.1 Modelling in ANSYS 15.0

The final model is designed in ANSYS 15.0 itself to overcome the contact problem faced in the simulation process, when the model is imported from CATIA V6 software and is designed in two steps i.e. modelling of bearing as per dimensions are shown above, modelling of the cage which is listed below.

I. Design of bearing

The design of bearing has been done in several steps which are listed in fig: 4.5 in the picture.

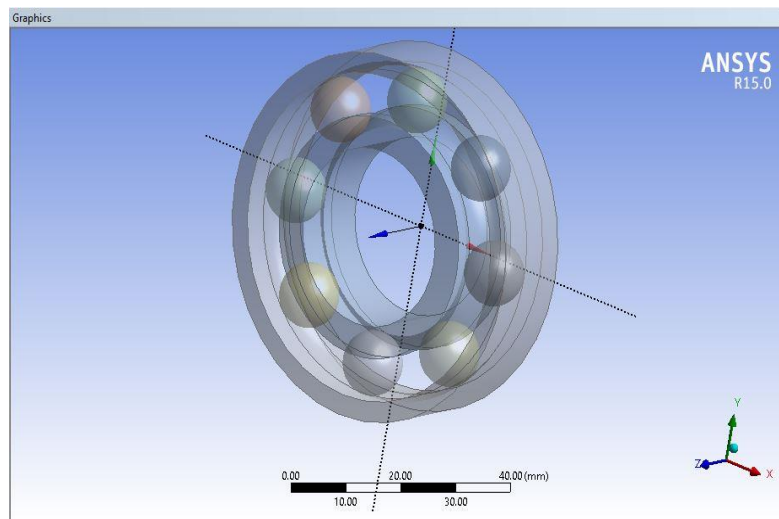


Figure 4.5: Model of bearing in ANSYS 15.0

II. Design of cage

Several cage geometries had tried, but some failed to rotate. Causes are:

- a) Having cylindrical surface on ball contact zone.
- b) Having a greater mass of cage balls were not making sufficient thrust force to rotate the cage.
- c) Having large no. of elements; there was a difficulty for the solver to solve the calculations requiring much more time.

The fourth design of cage was successfully mounted on a bearing which is listed in fig: 4.6.

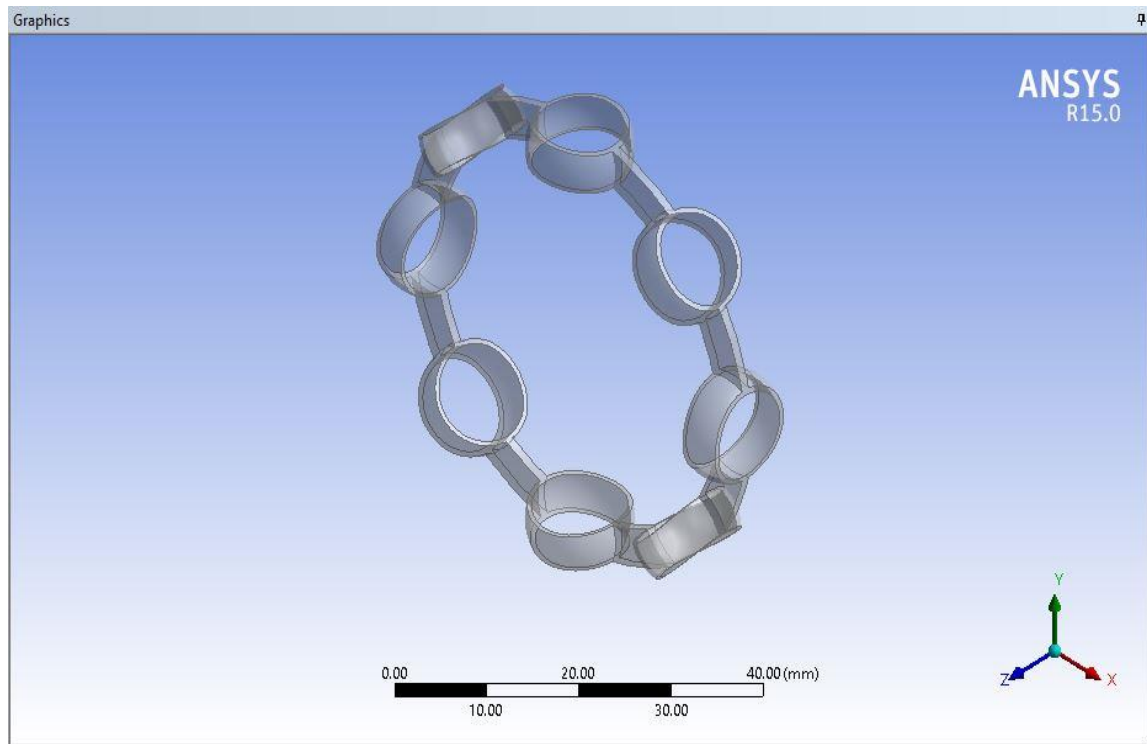


Figure 4.6: Final design of cage

Bearing Finalized model with cage is listed in fig: 4.7.

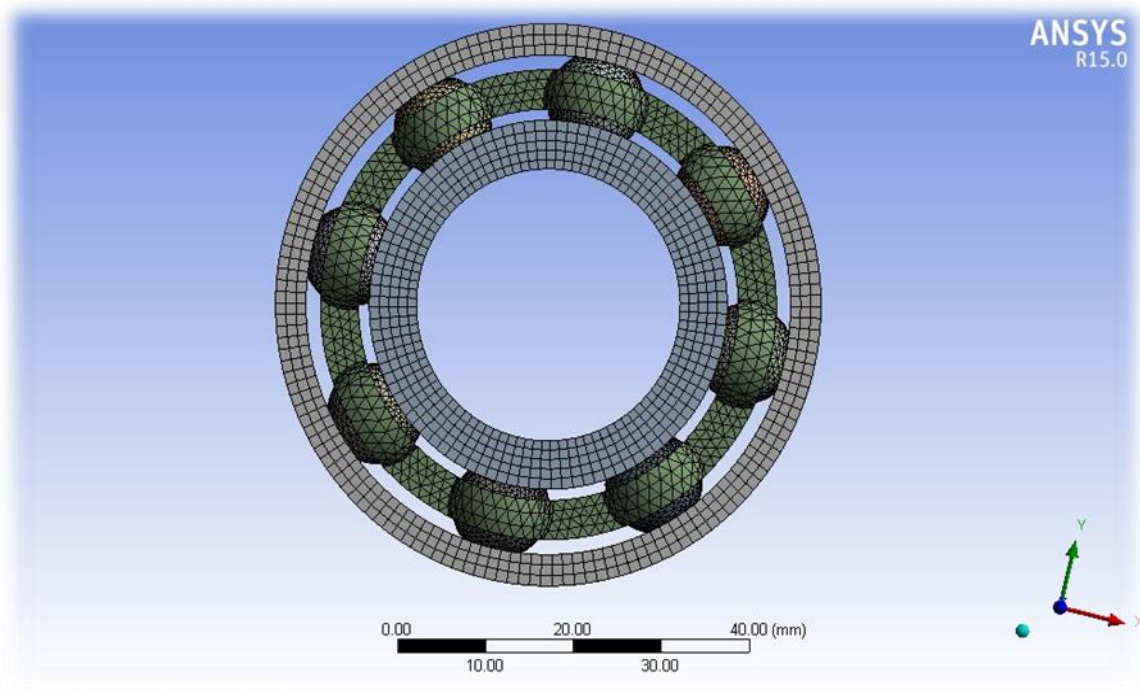


Figure 4.7: Final model of bearing in ANSYS 15.0

4.4 Support System

The three support system is designed for giving a radial load to the shaft. Step shaft is designed to reduce the elements and nodes which result in less usage of memory and CPU. The design of three support system followed by several steps which are listed in fig: 4.8,4.9.

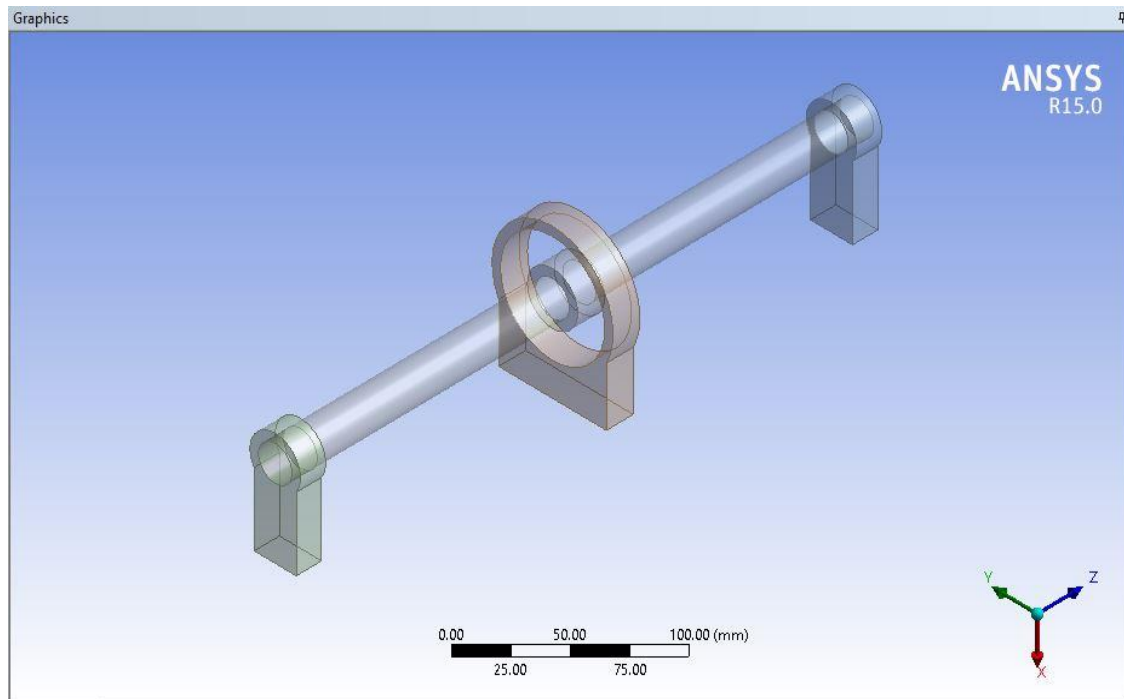


Figure 4.8: Modelling of three support system in ANSYS15.0

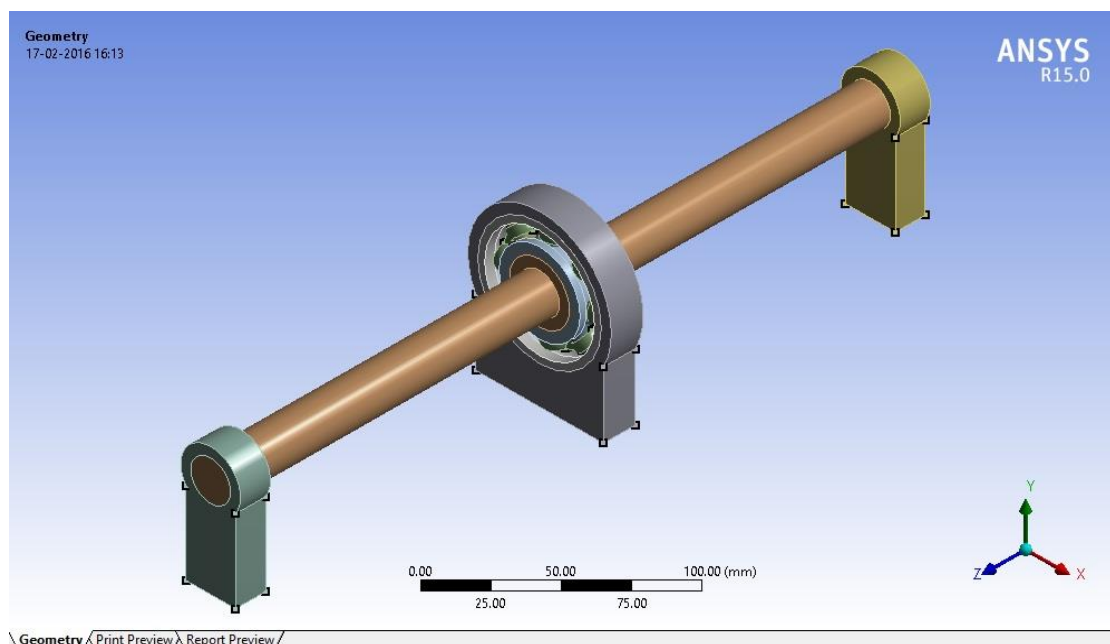


Figure 4.9: Final model of ball bearing setup with support system n ANSYS 15.0

4.5 Model Meshing in ANSYS 15.0

Model is meshed with different meshing control methods to improve the result and to make it compatible with memory and time limit. Steps that are followed to find the complete model meshing is listed in fig: 4.10.

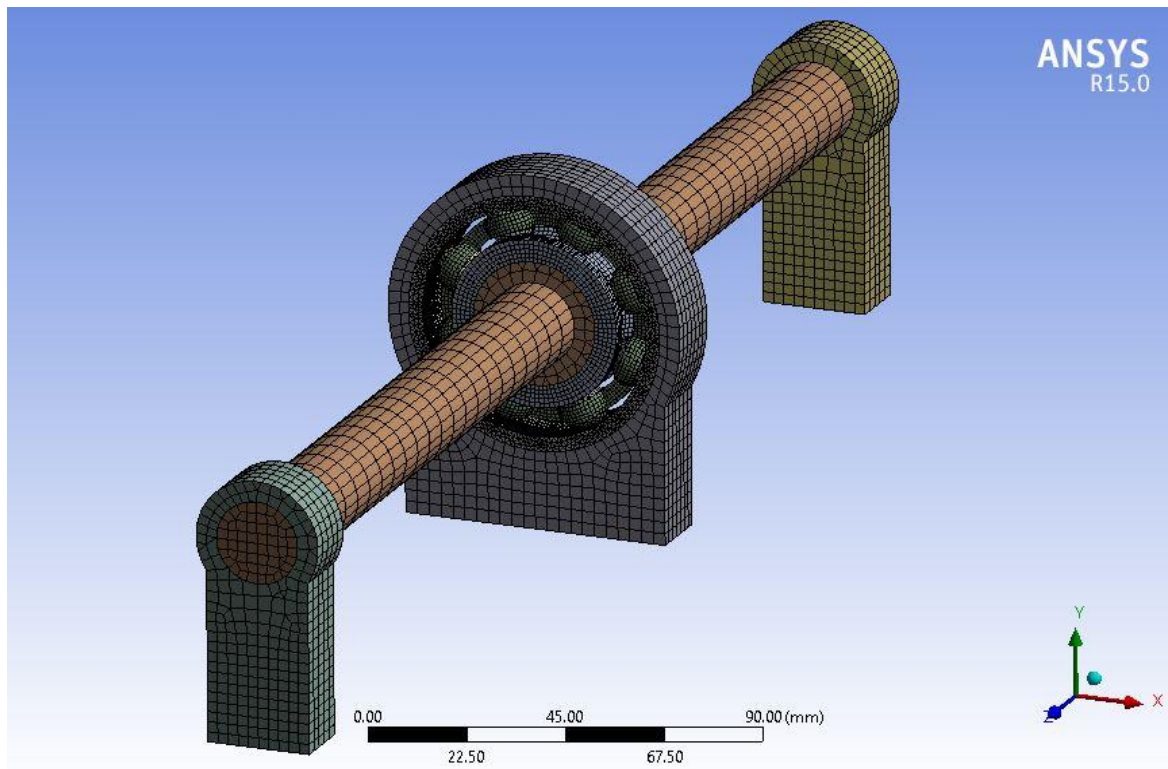


Figure 4.10: Model meshing in ANSYS15.0

4.6 Model with Crack

The second model (fig: 4.11) with a crack in the outer race inner surface which is in contact with balls has been prepared and is listed below. Crack width is 3mm and depth is 1mm in the y direction radially, at a distance of 28.5 mm to 29.5 mm and has made on the surface of the outer race, exposed to balls.

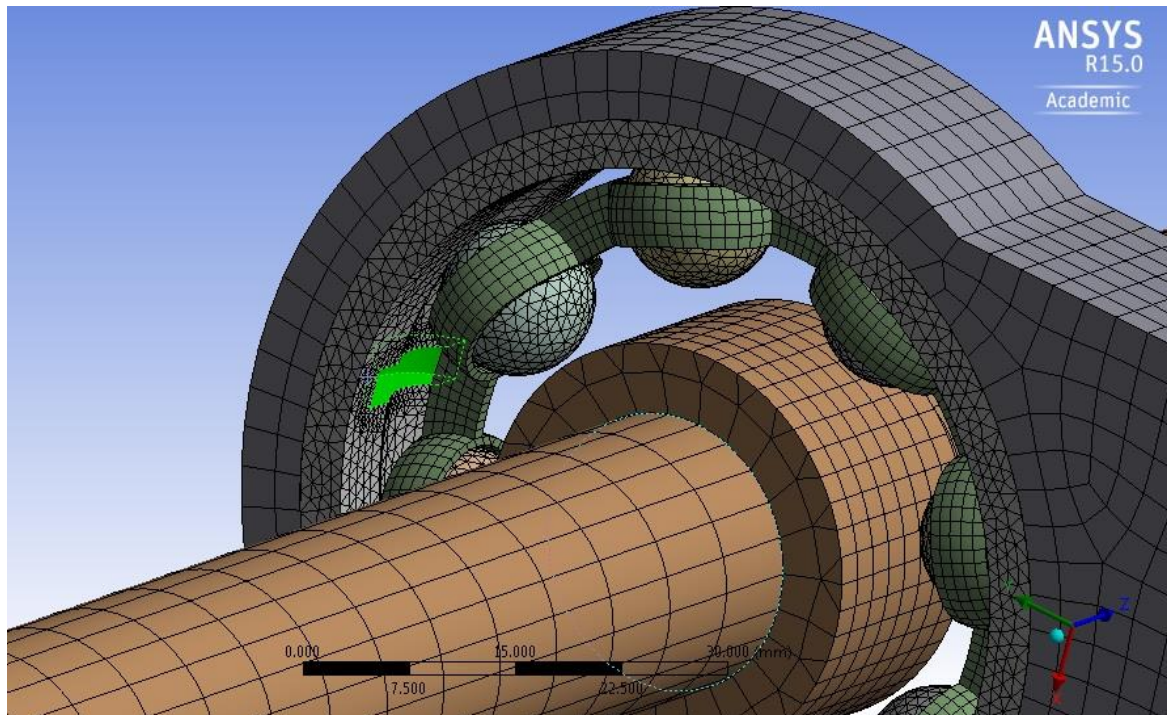


Figure 4.11: Second model (bearing with crack)

Chapter 5

Results and Discussion

When a healthy bearing without fault has been exposed to the dynamic analysis in ANSYS 15.0 and after 0.5 seconds data is captured from accelerometer probe. Five accelerometer probes have been placed on the sleeve which is shown in fig: 5.1.

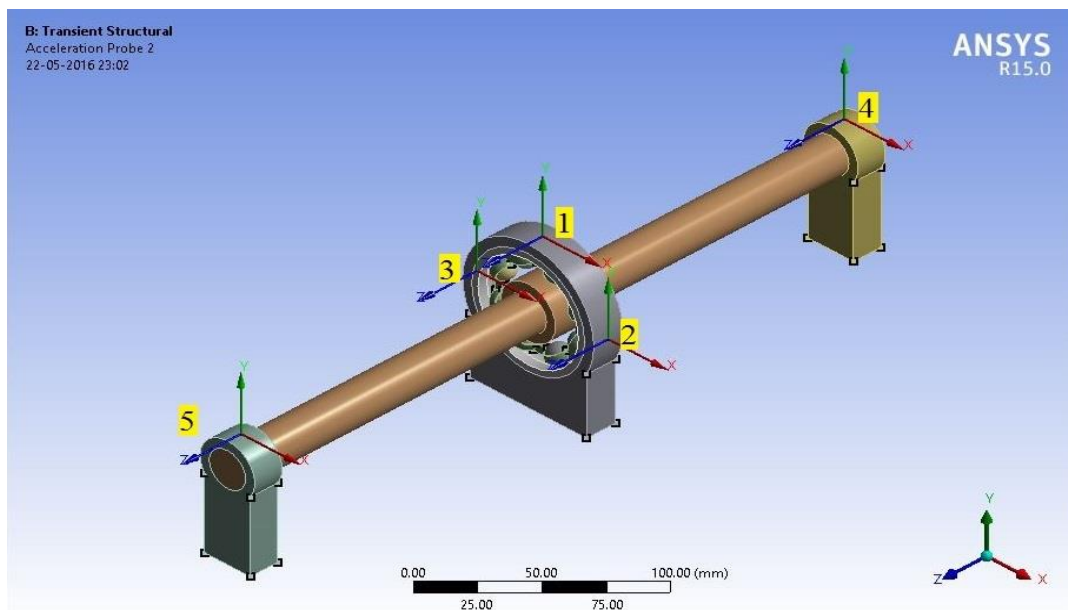


Figure 5.1: Positions of accelerometers probe in the model

From five accelerometers probes, data from probe one has been extracted which is exactly above the defect in Y- direction for both healthy and faulty bearing. Which shows the signals same as the signals obtained from numerical methods which are shown in fig: 5.2.

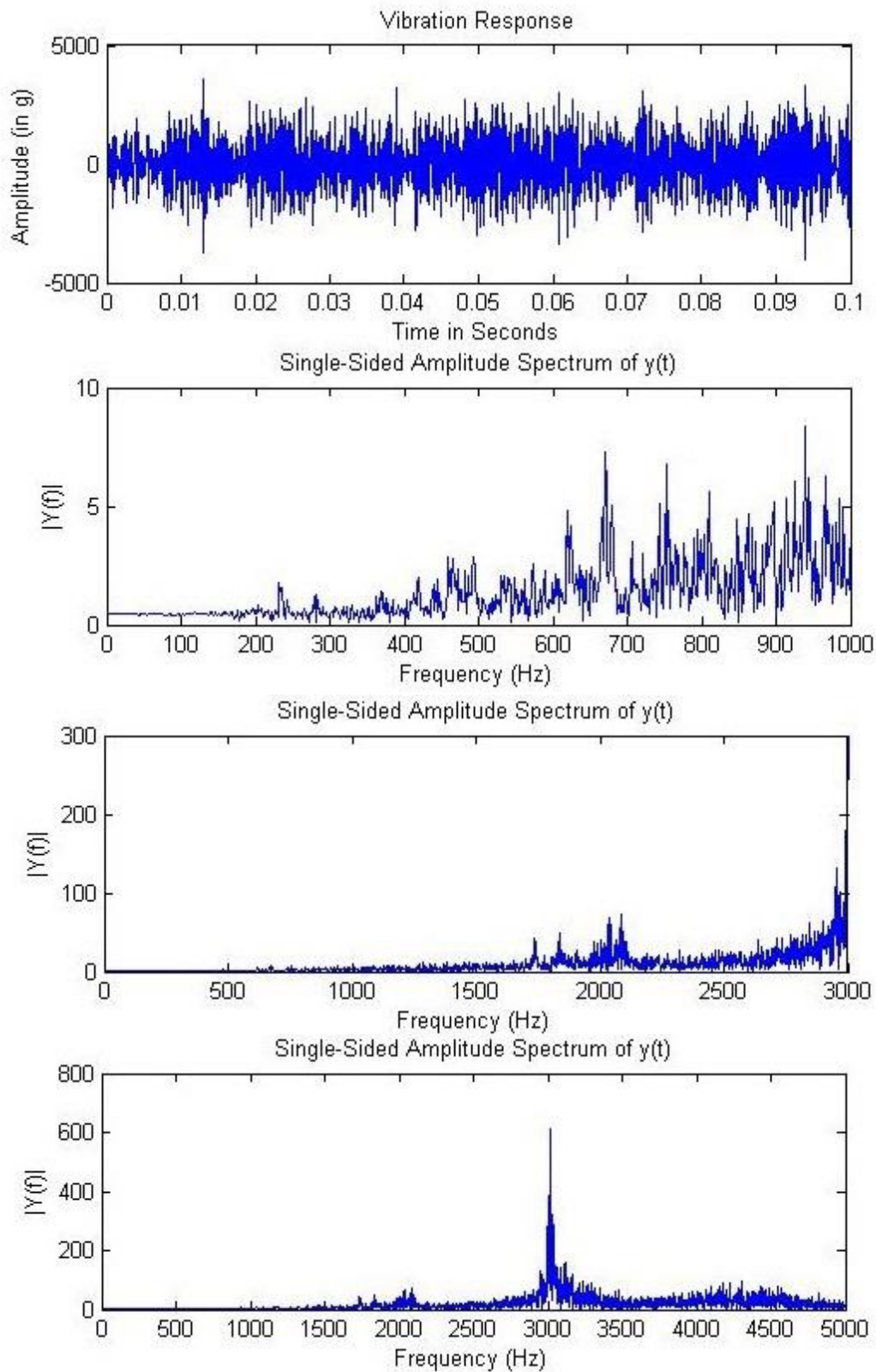


Figure 5.2: Vibration response of healthy bearing with frequency (1000,3000 and 5000 Hz)

An accelerometer shows a faulty signal when the ball passes through the known defect and is captured on the graph which is shown in fig: 5.3.

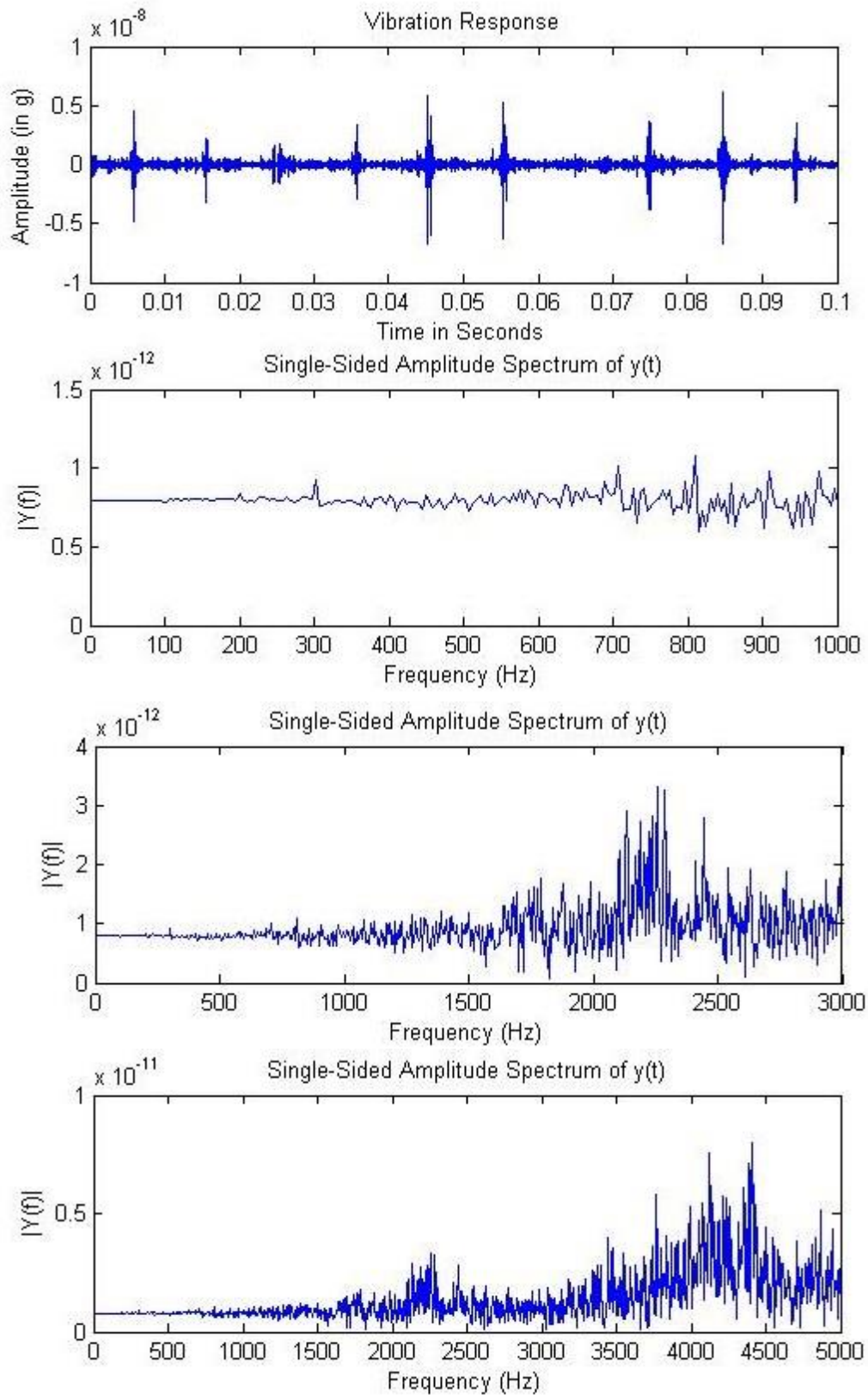


Figure 5.3: Vibration response of bearing with defect with frequency (1000,3000 and 5000 Hz)

Chapter 6

Conclusion

From the analysis mentioned above, following points can be summarized:

- Mesh density should be high in the contact zone that is in the outer race inner surface, inner race outer surface, ball surface and cage surface (exposed to balls). This will give the better results.
- The clearance between ball and cage plays a big role in finding vibration signals from the second model (with defect).
- Element size in the contact zone highly affects the time required for the simulation using finite element method. Therefore, element size of 1 mm is taken to generate the mesh in the contact zone.
- The bearing should be mounted on the shaft to giving a radial load to it.
- Contact type and friction coefficient are the most important parameters that should be taken into account.
- Cage is the necessary element for the rotation of the rolling element (balls) in deep groove ball bearing otherwise balls will get collapsed, and analysis will get stop.
- The result obtained from the analysis shows; this analysis has the capability to extract the vibration signal using ANSYS 15.0 workbench software. Hence, it can reduce the cost of testing as well as manufacturing of the bearing by optimization of the parameters of the bearing from this technique. Therefore, this analysis plays a big role in the field of testing and condition monitoring of the bearing. It opens a new area of research and in future, this analysis can be used to design and testing of a bearing which can successfully eliminate experimental testing.

6.1 Scope for Future Research

This analysis can be done on various bearings which are exposed to experimental testing before the used so that it can reduce the cost of testing and manufacturing.

References

1. Image: NYC 100-driving-axle-friction-bearing.jpg (2012) in Wikipedia. Available at: https://en.wikipedia.org/wiki/File:NYC_100-driving-axle-friction-bearing.jpg (Accessed: 1 May 2016).
2. Image: Deep groove ball bearing available at: http://img2.everychina.com/img/3b/05/945ba922e6026406507e0663b4b9-80x80c1-18dd/17x40x16_brass_cage_bearing_automobile_ball_bearings_steel_brass_nylon.jpg (Accessed: 1 May 2016).
3. Image: SKF Self-Aligning-Roller-Bearing available at: <http://image.made-in-china.com/2f1j00OMIQRiBGEJzw/SKF-Spherical-Roller-Bearings-Self-Aligning-Roller-Bearing-SKF-22316E-.jpg> (Accessed: 1 May 2016).
4. Image: Jewel bearing available at: <http://media.web.britannica.com/eb-media/33/110433-004-B50F01D3.gif> (Accessed: 1 May 2016).
5. Image: Elements of art color available at: <http://scripts.cac.psu.edu/jah5819/bearings/fluid.jpg> (Accessed: 20 May 2016).
6. Image: Radial magnet available at: <https://cdn.comsol.com/wordpress/2013/04/magnetic-bearings-axial-permanent-magnet-bearing.png> (Accessed: 2 May 2016).
7. Image: Open tic tac box available at: https://upload.wikimedia.org/wikipedia/commons/c/c7/Mint_box_polypropylene_lid.JPG (Accessed: 20 May 2016).
8. Image: Spherical roller thrust bearings, automotive, roller high, available at: <http://www.deepgroveballbearing.com/wp-content/uploads/deep-groove-ball-bearing-structure.jpg> (Accessed: 9 May 2016).
9. A, S. A., G, D. R., G, K. S., & Engineering, M. (2014). Theoretical and Experimental Studies on Vibrations Produced By Defects in Double Row Ball Bearing Using Response Surface Method, *3*(5), 140–145.
10. Bajaj, V. R., & Student, M. E. C. A. D. C. A. M. (2015). Finite Element Analysis of Integral Shaft Bearing, *3*(1), 28–36.
11. Graney, B. P., & Starry, K. (2011). Rolling element bearing analysis crosses threshold. *Materials Evaluation*, *70*(1), 78–85.

12. Kharche, P. P. (2014). Review of Fault Detection in Rolling Element Bearing. *International Journal of Innovative Research in Advanced Engineering*, 1(5), 169–174.
13. Pandiyarajan, R., Starvin, M. S., & Ganesh, K. C. (2012). Contact Stress Distribution of Large Diameter Ball Bearing Using Hertzian Elliptical Contact Theory. *Procedia Engineering*, 38, 264–269.
14. Saruhan, H., Sandemir, S., Çiçek, A., & Uygur, I. (2014). Vibration Analysis of Rolling Element Bearings Defects. *Journal of Applied Research and Technology*, 12(3), 384–395.
15. Sheen, Y. T. (2004). A complex filter for vibration signal demodulation in bearing defect diagnosis. *Journal of Sound and Vibration*.
16. Shiroishi, J., Li, Y., Liang, S., Kurfess, T., & Danyluk, S. (1997). Bearing condition diagnostics via vibration and acoustic emission measurements. *Mechanical Systems and Signal Processing*, 11(5), 693–705.
17. Image: Available at: <http://divestmergeacquire.com/wp-content/uploads/574/Coiled-Spring-Web-e1460093418604.png> (Accessed: 19 May 2016).
18. Image: Retrieved from ANSYS 15.0 help (article: Nonlinearity)
19. Image: Retrieved from ANSYS 15.0 help (article: Nonlinearity)
20. Image: Stress-strain curve for ductile available at: <http://4.bp.blogspot.com/-XmQJ-Rsqp1c/UV6fxMB9M5I/AAAAAAAAAGA/u8PzM99-ruI/s1600/kurva.png> (Accessed: 21 May 2016).
21. Image: Dimensions of SKF W 6206-2Z bearing. Available at: <http://www.skf.com/in/products/bearings-units-housings/ball-bearings/deep-groove-ball-bearings/stainless-steel-deep-groove-ball-bearings/single-row-stainless-steel/index.html?designation=W%206206-2Z> (Accessed: 26 May 2016).

Annexure – A

Modelling

Modelling starts through Double clicking on the Geometry in the Toolbox, and it appears on the Project Schematic window. The next step is to open the Design Modeler by double clicking on the Geometry in the second row of the project schematic window, where a question mark appears (fig: A.1).

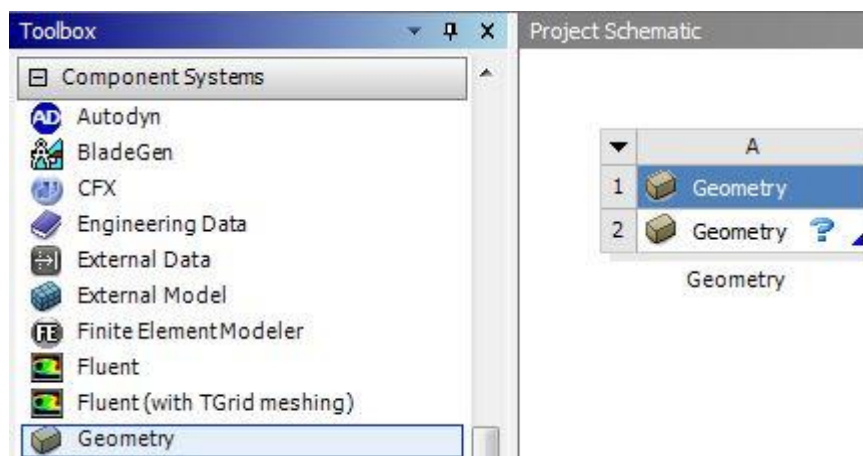


Figure A.1: Toolbox of ANSYS 15.0

Next step is to work on design modeler by using various primitives and other tools defined in ANSYS 15.0 Design Modeler. There are nine primitives defined in ANSYS 15.0 which can be used directly to create a shape which is shown in fig: A.2.



Figure A.2: Primitives defined in ANSYS 15.0

So the first step of modelling starts with the designing of the outer race. Which can be done by two ways. First way of designing is to use the sketching tools and second way is to entering the primitives. In this modelling work, second way has been preferred to model the bearing. The first primitive (cylinder) has been entered for the outer race designing. Which is entered by clicking on the **Create** icon then go to **Primitives** and select **Cylinder**. The pictorial representation is shown in fig: A.3.

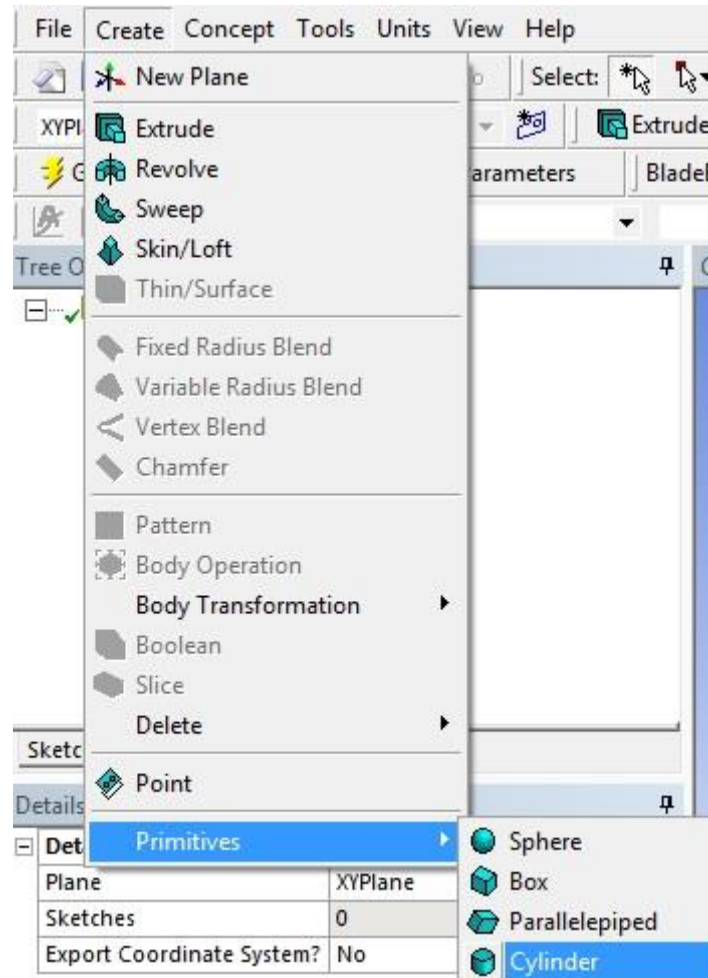


Figure A.3: Inserting a primitive (cylinder)

After this, it appears in the **Tree Outline** window in the left now go to the **Details** window and set **Operation** as **Add Frozen** and the dimensions in **Axis Definition** as **X component 0 mm, Y component 0 mm, Z component 16 mm** and **Radius 31 mm** (fig: A.4 (a)) and it appears (fig: A.4 (b)) on the **Graphics** window as shown in fig: A.4.

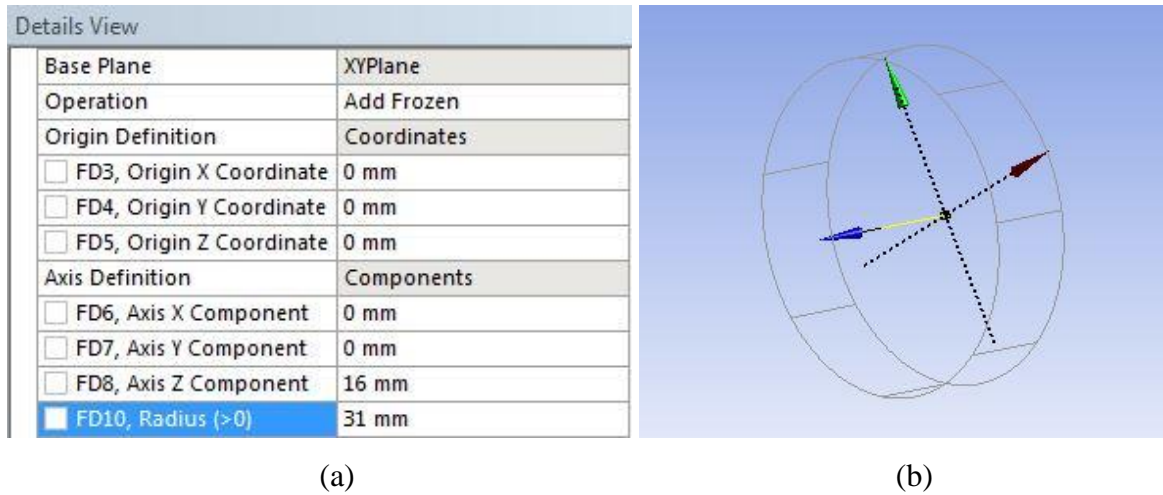


Figure A.4: Axis definition (a) and graphics of cylinder (b)

Next is to click on **Generate** icon (fig: A.5 (a)) and it appears in the **Graphics** window (fig: A.5 (b)) as a solid model.

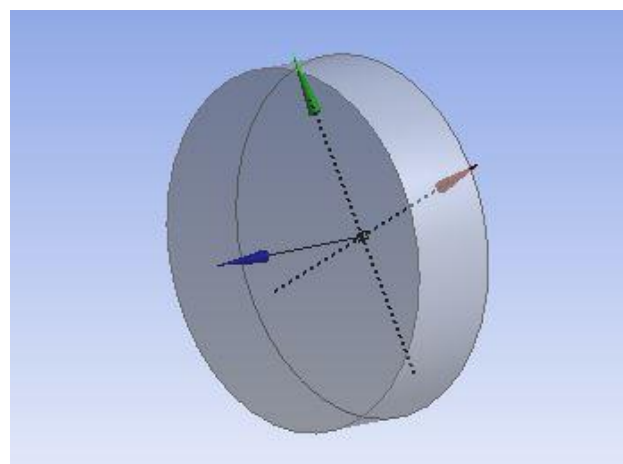
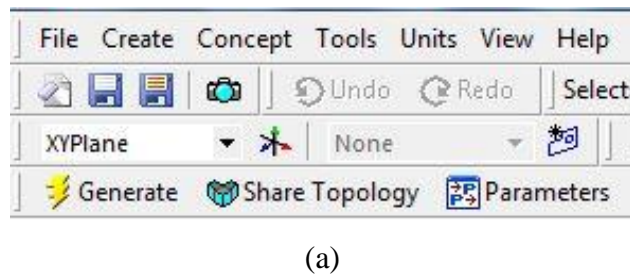


Figure A.5: Position of generate icon (a) and graphics of cylinder (b)

Next step is to insert a new cylinder similarly as previous and set **Operation** as **Add Frozen** and the dimensions in **Axis Definition** as **X component 0 mm, Y component 0 mm, Z component 30 mm** and **Radius 27.5 mm** (fig: A.6 (a)) and on clicking the **Generate** icon it appears (fig: A.6 (b)) in the **Graphics** window.

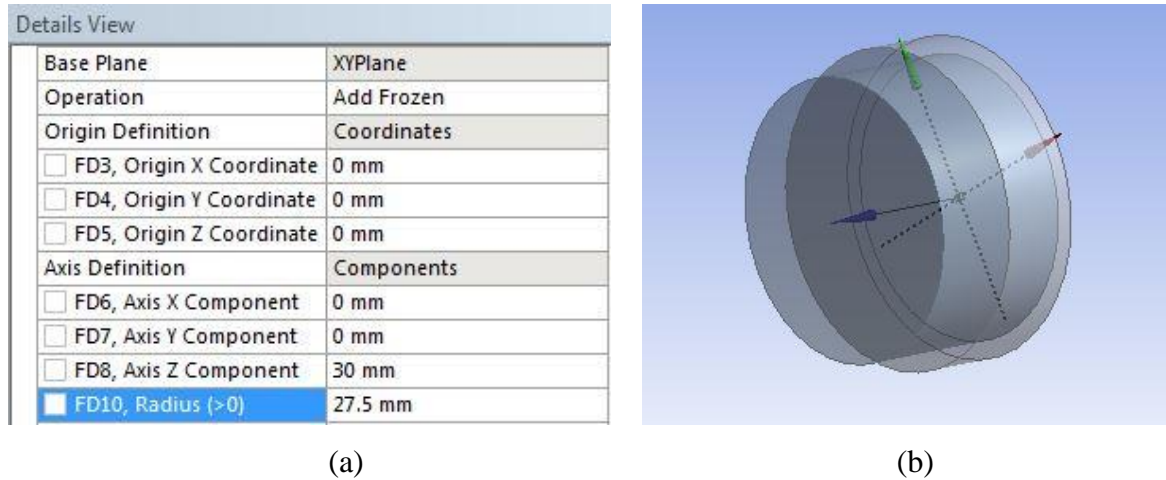
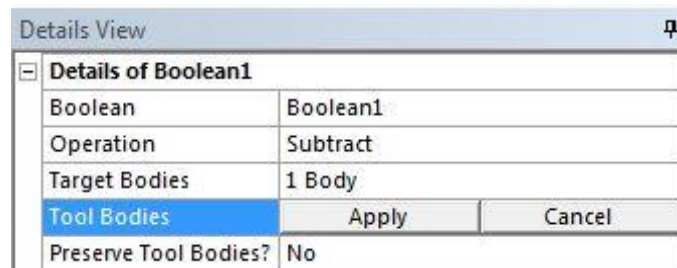
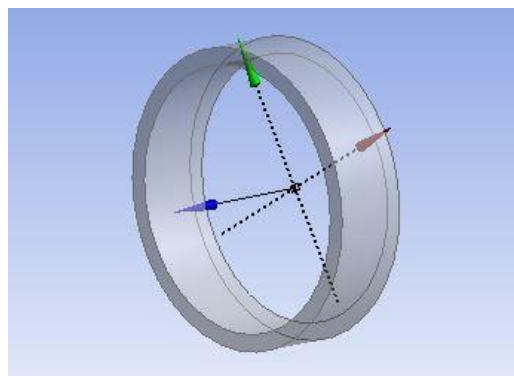


Figure A.6: Axis definition (a) and graphics of cylinder (b)

In the next step, go to create icon and select boolean and then go to details window and select **Operation** as **Subtract Target Bodies** as cylinder 1 and **Tool Bodies** as Cylinder 2 (on Graphics window) and **Apply** (fig: A.7 (a)). Go to the **Generate** icon and select to generate the resulting body, which appears in the **Graphics** window (fig: A.7 (b)).



(a)



(b)

Figure A.7: Details view (a) and Graphics of boolean (b)

Similarly, insert a new cylinder from primitives and set **Operation** as **Add Frozen** and the dimensions in **Axis Definition** as **X component 0 mm, Y component 0 mm, Z component 16 mm** and **Radius 20.35 mm** and on clicking the **Generate** icon it appears on the **Graphics** window as shown in fig: A.8.

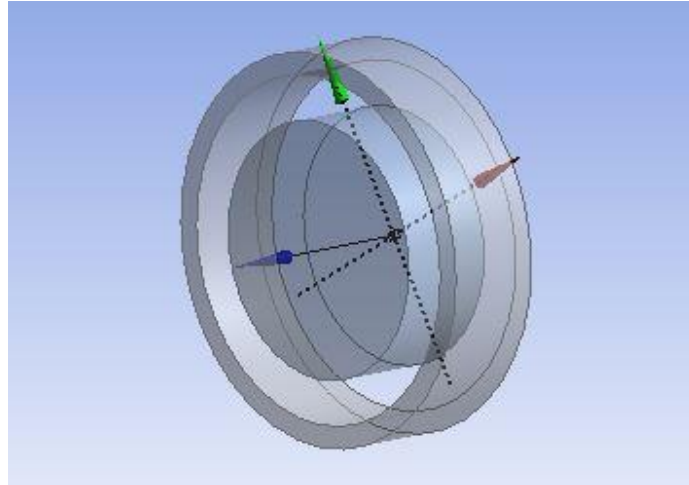


Figure A.8: Graphics of cylinder

Next is to insert a new cylinder from primitives and set **Operation** as **Add Frozen** and the dimensions in **Axis Definition** as **X component 0 mm, Y component 0 mm, Z component 30 mm** and **Radius 15 mm** and on clicking the **Generate** icon it appears on the **Graphics** window as shown in fig: A.9.

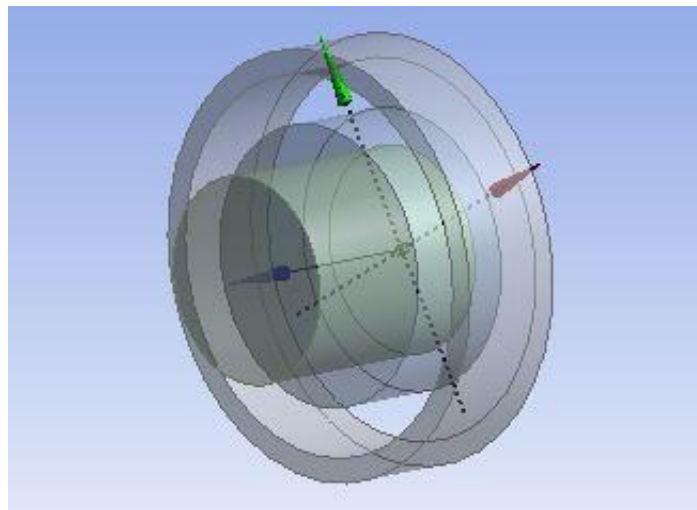


Figure A.9: Graphics of cylinder

The next step is to subtract cylinder 4 from cylinder 3 for designing of inner race. For this task insert boolean and then go to Details window and Select **Operation** as **Subtract** **Target Bodies** as cylinder 3 and **Tool Bodies** as Cylinder 4 (on Graphics window) and

Apply. Go to the **Generate** icon and click to generate the resulting body, which appears in the **Graphics** window (fig: A.10).

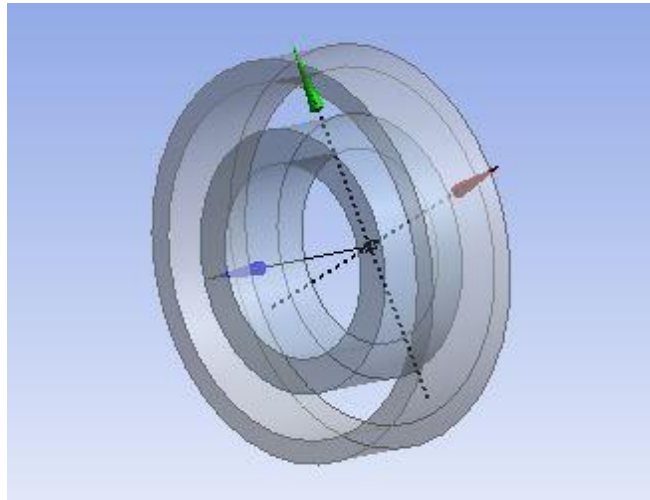
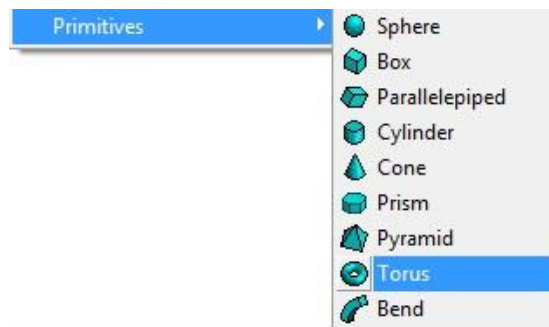


Figure A.10: Graphics of boolean

Next is to insert a **Torus** from **Primitives** (fig: A.11 (a)) and then go to the **Details** window and set **Operation** as **Add Frozen**, define **Origin X Coordinate 0 mm**, **Origin Y Coordinate 0 mm** and **Origin Z Coordinate 8 mm** (fig: A.11 (b)), **Inner Radius 17.5 mm** and **Outer Race 28.5 mm** in **Base Definition** (fig: A.11 (c)).



(a)

Details View	
Details of Torus1	
Torus	Torus1
Base Plane	XYPlane
Operation	Add Frozen
Origin Definition	Coordinates
<input type="checkbox"/> FD3, Origin X Coordinate	0 mm
<input type="checkbox"/> FD4, Origin Y Coordinate	0 mm
<input checked="" type="checkbox"/> FD5, Origin Z Coordinate	8

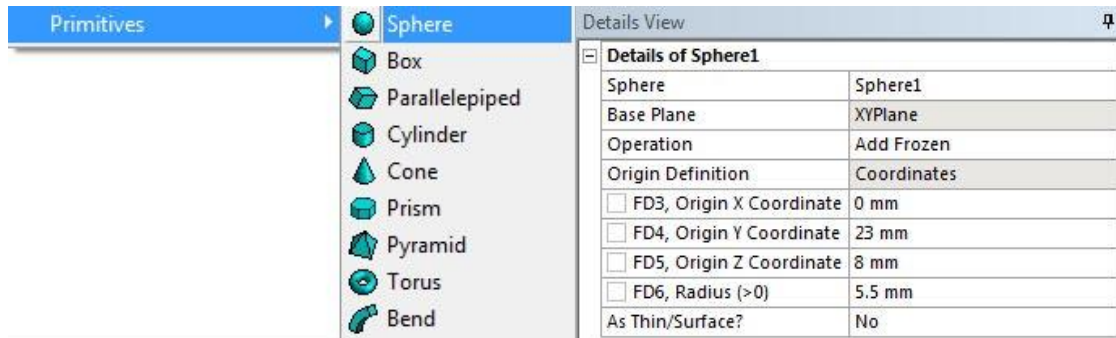
(b)

Base Definition	Components
<input type="checkbox"/> FD9, Base X Component	0
<input type="checkbox"/> FD10, Base Y Component	1
<input type="checkbox"/> FD11, Base Z Component	0
<input type="checkbox"/> FD12, Angle (>0)	360 °
<input type="checkbox"/> FD13, Inner Radius (>0)	17.5 mm
<input checked="" type="checkbox"/> FD14, Outer Radius (>0)	28.5 mm
As Thin/Surface?	No

(c)

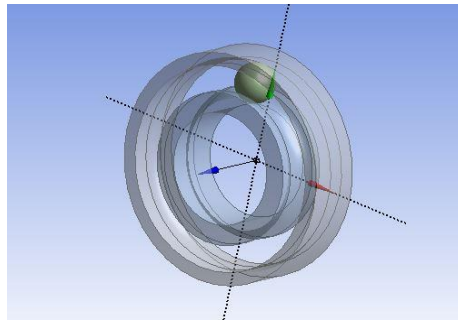
Figure A.11: Insert torus (a), Details view (b) and Base definition (c)

Next step is to insert a **Sphere** from **Primitives** (fig: A.12 (a)) and then go to the **Details** window and set **Operation** as **Add Frozen**, define **Origin X Coordinate 0 mm**, **Origin Y Coordinate 23 mm**, **Origin Z Coordinate 8 mm** in and **Radius 5.5 mm** in **Origin Definition** (fig: A.12 (b)) and it appears in the **Graphics** window as shown in (fig: A.12 (c)).



(a)

(b)



(c)

Figure A.12: Insert sphere (a), Details view (b) and graphics of the geometry (c)

Then select **ZX Plane** in the tree and go to the **Sketching** module and select a **line** and **draw** it on **z axis** then go to **constraints** and select **coincident** and by pressing the control button to select the **line** and **Z- axis**. Now it appears under the **ZX Plane** as **Sketch 1** in the tree (fig: A.13).

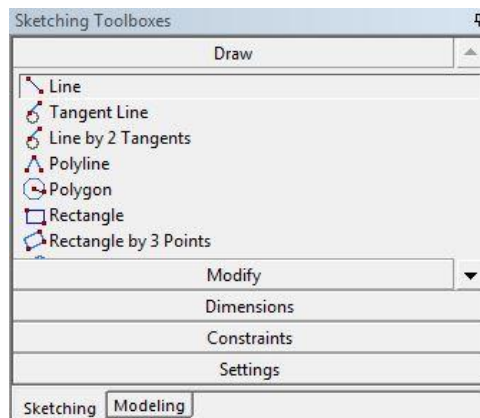
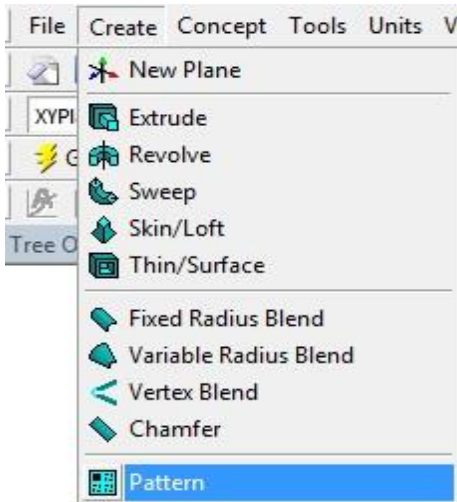
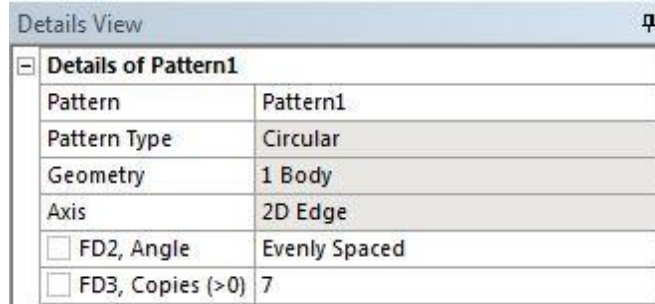


Figure A.13: Sketching toolbox

Now insert **Pattern** (fig: A.14 (a)) from **Create** icon as shown below and select **Pattern Type** as **Circular, Angle – Evenly Spaced and Copies – 7** (fig: A.14 (b)).

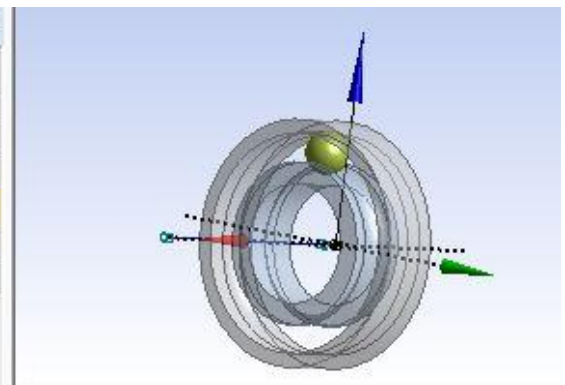
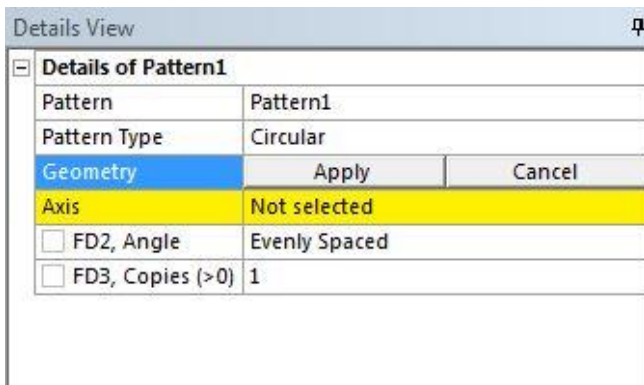


(a)

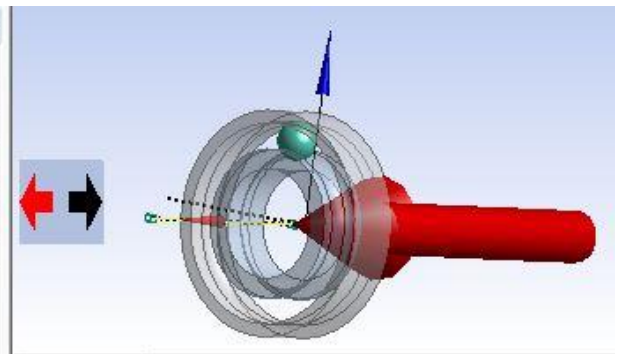
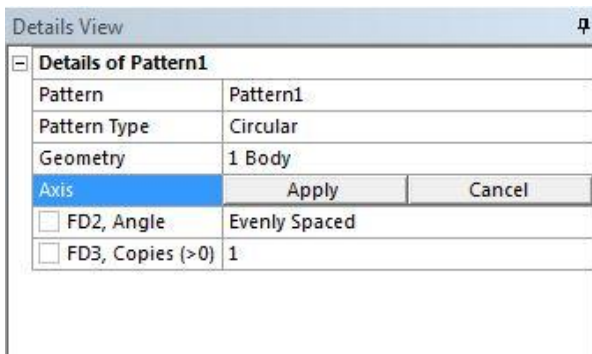


(b)

Then click on **Geometry** and select body as ball (fig: A. 14 (c)) and **Axis** as **Sketch 1** (fig: A.14 (d)).



(c)



(d)

Figure A.14: Insert pattern (a), Details view (b), Geometry selection (c), Axis selection (d)

On generating it shows a pattern of 8 balls around Z-axis which is shown in fig: A.15.

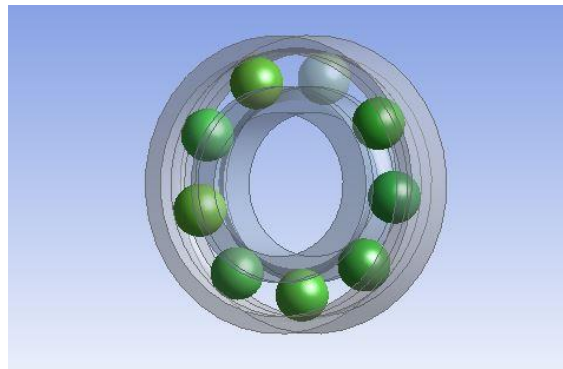


Figure A.15: Graphics view of pattern

For designing the cage, the following steps have been followed.

Insert a Cylinder and set **Operation** as **Add Frozen** and the dimensions in **Origin Definition** as **X Coordinate 0 mm, Y Coordinate 0 mm, Z Coordinate 7.5 mm** and **Axis Definition** as **X component 0 mm, Y component 0 mm, Z component 1 mm** and **Radius 25.91 mm** and then click on the Generate icon. Similarly, enter another cylinder with **Origin Definition** as **X Coordinate 0 mm, Y Coordinate 0 mm, Z Coordinate 7.5 mm** and **Axis Definition** as **X component 0 mm, Y component 0 mm, Z component 3 mm** and **Radius 21.59 mm** and **Generate**. Then enter **Boolean** and set **Operation** as **Subtract** and select **Target Bodies** as Cylinder 5 and **Tool Bodies** as Cylinder 6 and then **Generate**. On suppressing all bodies above cylinder 5, it looks like as shown in fig: A.16.

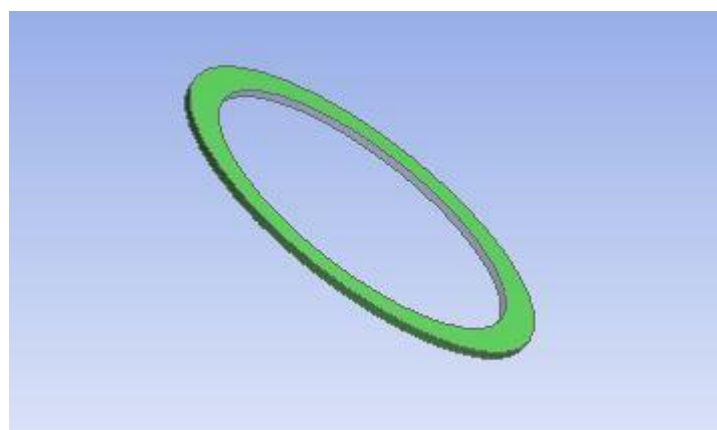
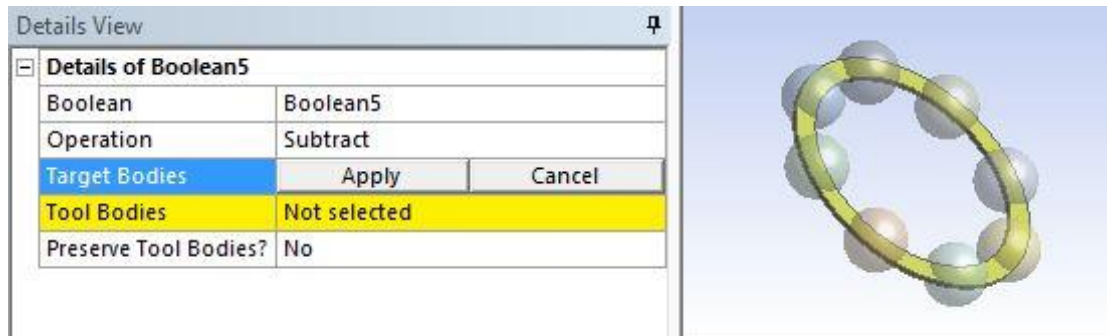


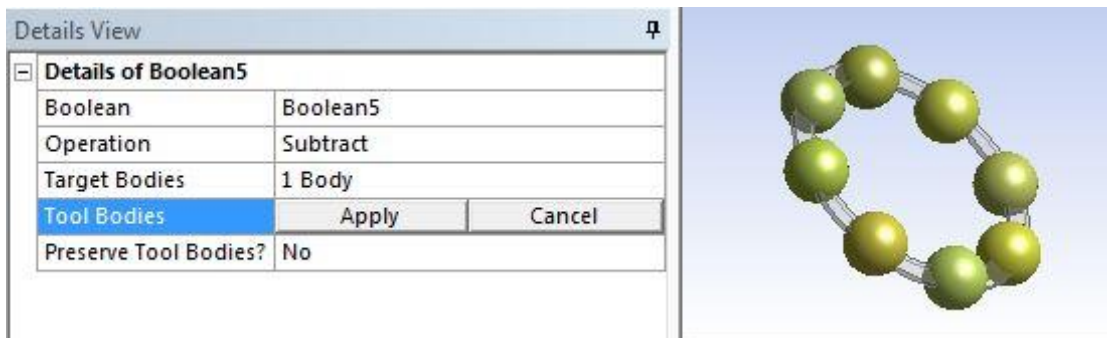
Figure A.16: Graphics view of cage ring

Next is to insert a **Sphere** from **Primitives** and then go to the **Details** window and set **Operation** as **Add Frozen**, define **Origin X Coordinate 0 mm, Origin Y Coordinate 23 mm,**

Origin Z Coordinate 8 mm in and **Radius 6 mm** in **Origin Definition** and similarly **pattern** it in a **circular** manner with respect to the **Sketch 1** and make **7 copies**. Then insert **Boolean** and set **Operation** as **Subtract**, **Target bodies** as the ring (fig: A.17 (a)) and **Tool Bodies** as eight balls (fig: A.17 (b)).



(a)



(b)

Figure A.17: Target bodies selection (a) and Tool bodies selection (b)

Then click on Generate icon and it looks like shown in the fig A.18.

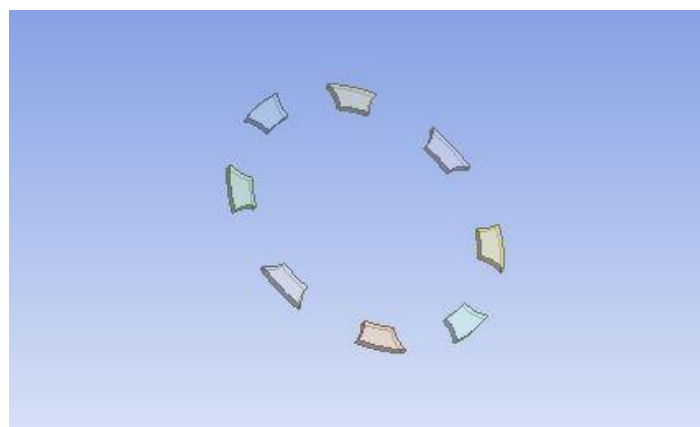


Figure A.18: Boolean of cage ring

Next step is to insert a **Sphere** from **Primitives** and then go to the **Details** window and set **Operation** as **Add Frozen**, define **Origin X Coordinate 0 mm**, **Origin Y Coordinate 23 mm**, **Origin Z Coordinate 8 mm** in and **Radius 6 mm** in **Origin Definition** and similarly pattern it in a circular manner with respect to the Sketch 1 and make 7 copies and Generate. It looks like the fig: A.19.

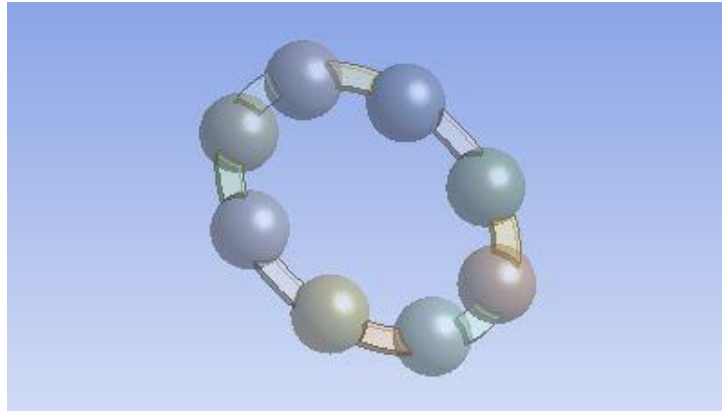


Figure A.19: Pattern of cage balls

In the next step insert a new cylinder from primitives and set **Operation** as **Add Frozen** and the dimensions in **Axis Definition** as **X component 0 mm**, **Y component 0 mm**, **Z component 30 mm** and **Radius 21.59 mm** and on clicking the **Generate** icon it appears on the **Graphics** window as shown in fig: A.20.

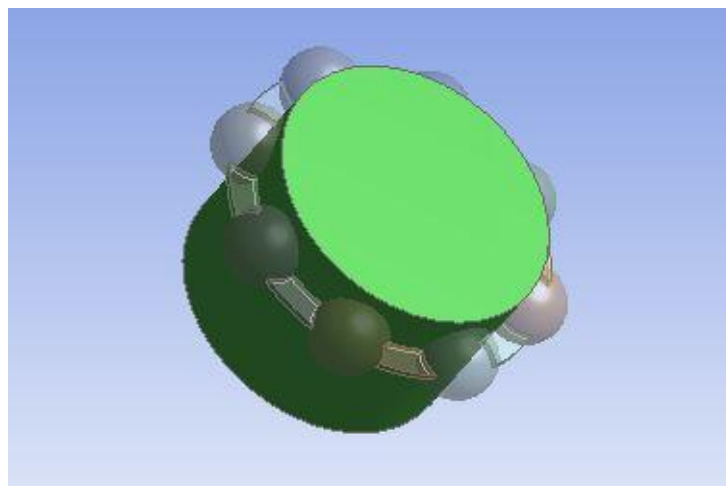
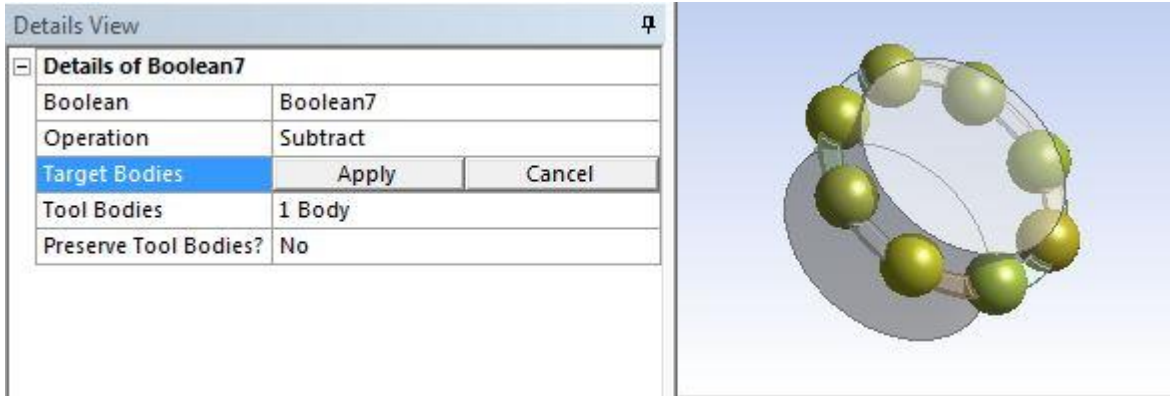
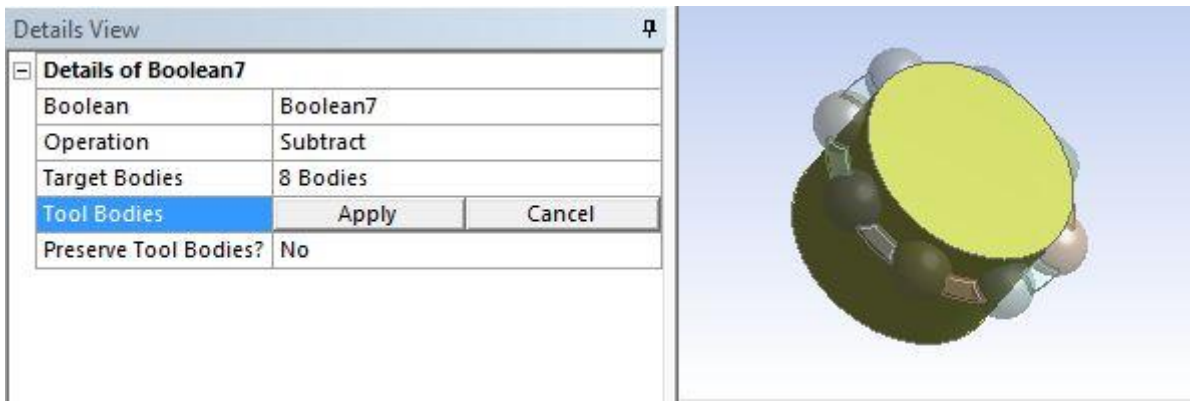


Figure A.20: Inserting a cylinder

Then insert **Boolean** and set **Operation** as **Subtract**, **Target bodies** as eight balls (fig: A.21 (a)) and **Tool Bodies** as cylinder 7 (fig: A.21 (b)).



(a)



(b)

Figure A.21: Target bodies selection (a) and Tool bodies selection (b)

Then click on Generate icon and it looks as shown in fig: A.22.

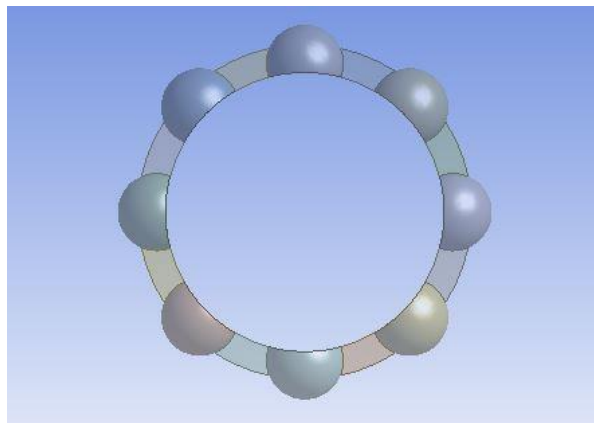


Figure A.22: Graphics of Boolean

Then insert two cylinders from primitives and set **Operation** as **Add Frozen** and the dimensions in **Axis Definition** as **X component 0 mm, Y component 0 mm, Z component**

18 mm and **Radius 35 mm** for Cylinder 8 and **X component 0 mm, Y component 0 mm, Z component 30 mm** and **Radius 25.91 mm** for Cylinder 9. It looks like as shown in fig: A.23.

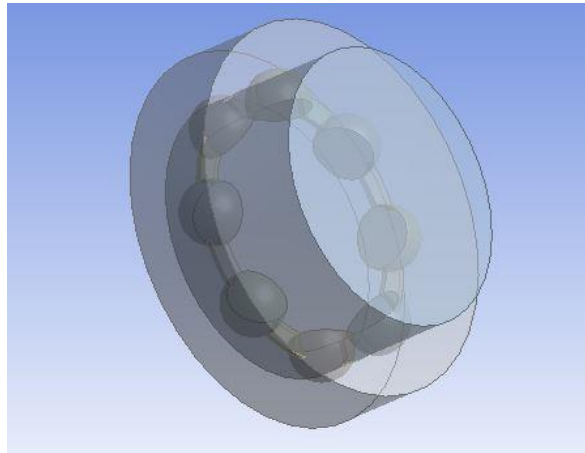
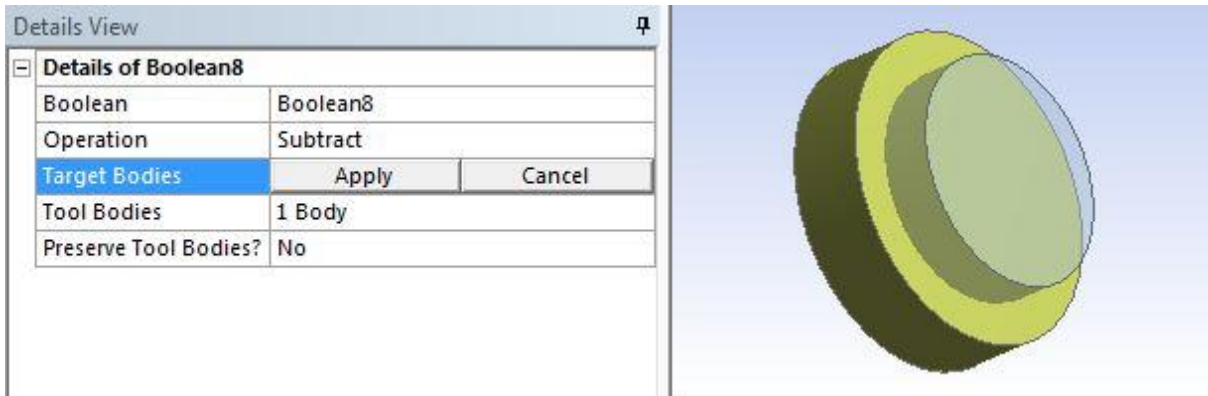
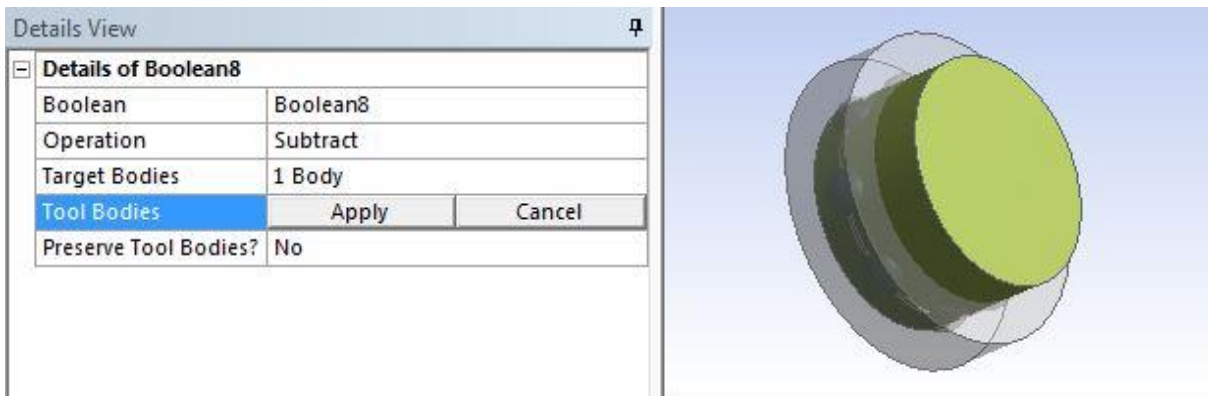


Figure 23: Inserting two cylinders

Then insert **Boolean** and set **Operation** as **Subtract**, **Target bodies** as cylinder 8 (fig: A.24 (a)) and **Tool Bodies** as cylinder 9 (fig: A.24 (b)).



(a)



(b)

Figure A.24: Target bodies selection (a) and Tool bodies selection (b)

Then click on Generate and it looks like a ring as shown in the fig: A.25.

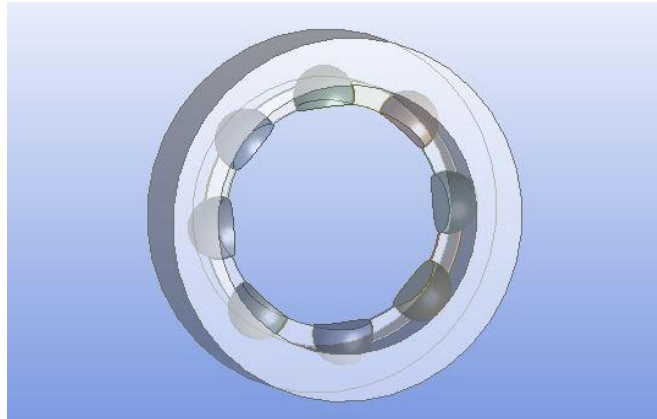
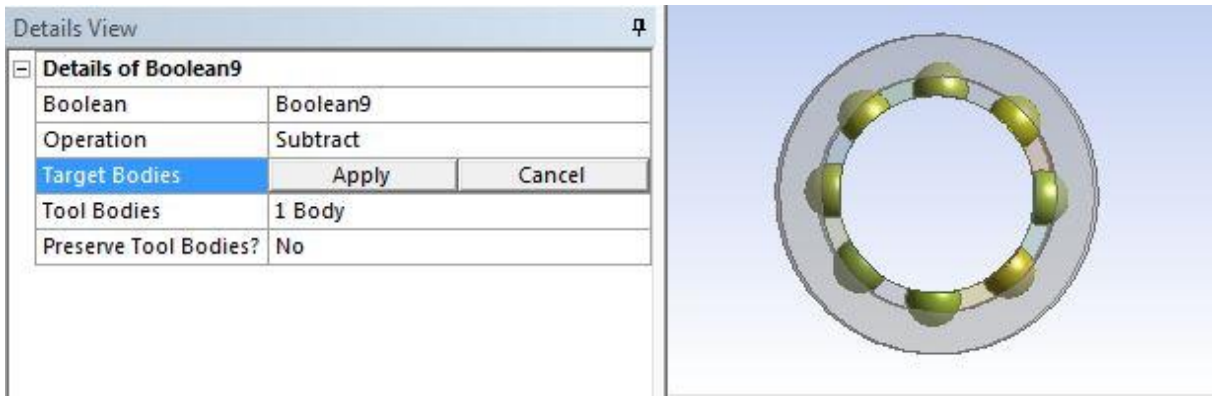
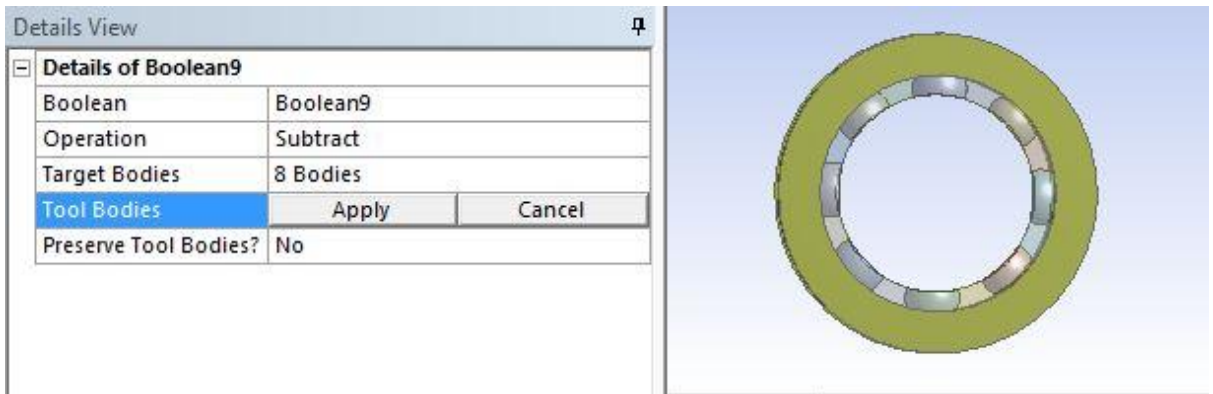


Figure A.25: Graphics of boolean

Then insert another **Boolean** and set **Operation** as **Subtract**, **Target bodies** as eight balls (fig: A.26 (a)) and **Tool Bodies** as the ring (fig: A.26 (b)) generated above this step.



(a)



(b)

Figure A.26: Target bodies selection (a) and Tool bodies selection (b)

Then click on Generate and the resulting bodies on Graphics window looks like fig: A.27.

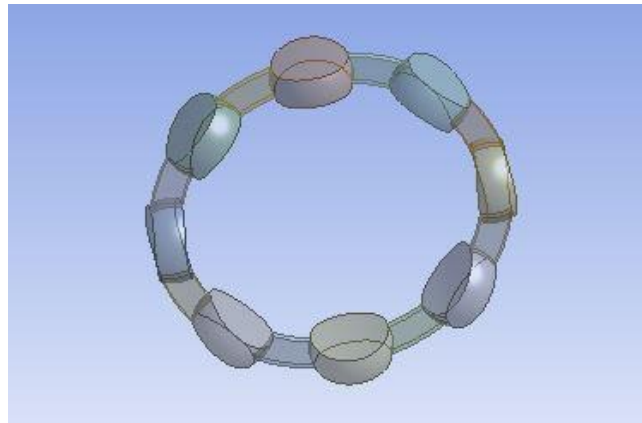


Figure A.27: Graphics of boolean

Next step is to insert a **Sphere** from **Primitives** and then go to the **Details** window and set **Operation** as **Add Frozen**, define **Origin X Coordinate 0 mm**, **Origin Y Coordinate 23 mm**, **Origin Z Coordinate 8 mm** in and **Radius 5.52 mm** in **Origin Definition** and similarly pattern it in a circular manner with respect to the Sketch 1 and make 7 copies and Generate. It looks like in the fig: A.28.

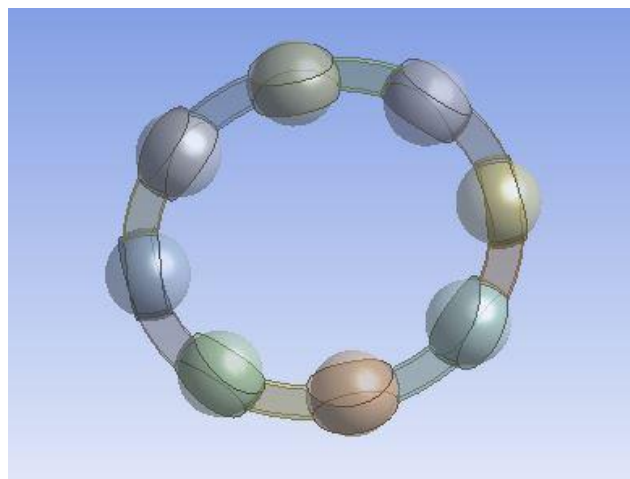
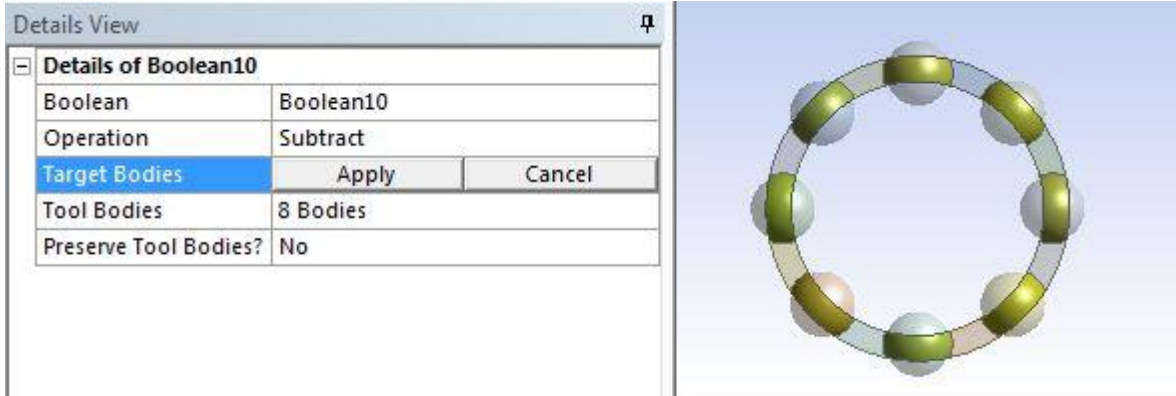
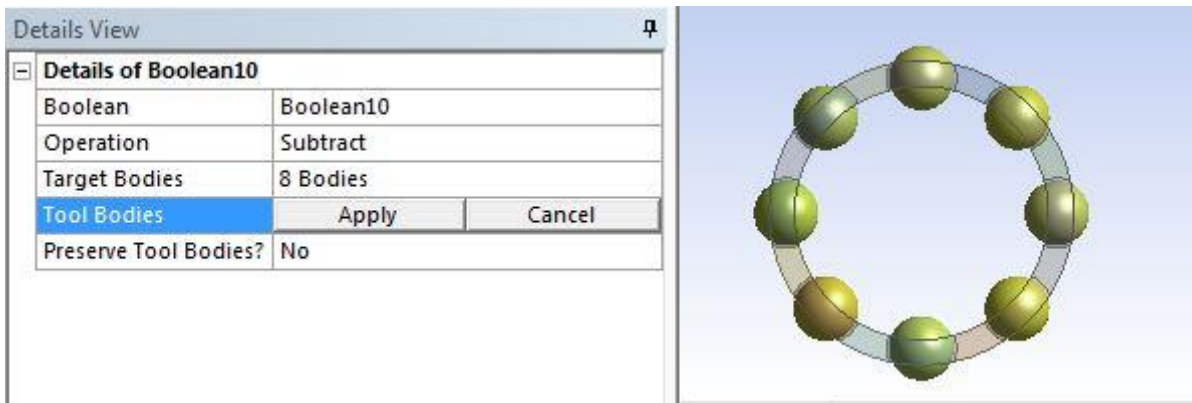


Figure A.28: Inserting sphere and pattern

Then insert another **Boolean** and set **Operation** as **Subtract**, **Target bodies** as ring (fig: A.29 (a)) and **Tool Bodies** as eight balls (fig: A.29 (b)) generated above this step.



(a)



(b)

Figure A.29: Target bodies selection (a) and Tool bodies selection (b)

Then on Generating, it looks like the complete cage as shown fig: A.30.

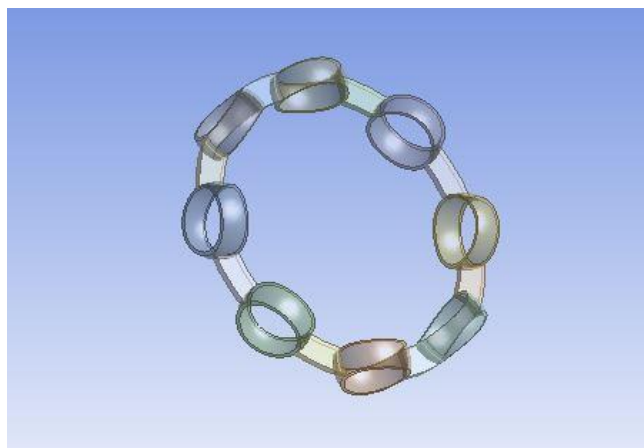


Figure A.30: Final design of cage

Then **Unsuppress** all bodies and modelling of the bearing is completed.